Received: 11 September 2019 | Revised: 7 February 2020 | Accepted: 13 February 2020

DOI: 10.1096/fj.201902331R

RESEARCH ARTICLE

THE FASEB JOURNAL

Systemic long-term inactivation of hypoxia-inducible factor prolyl 4-hydroxylase 2 ameliorates aging-induced changes in mice without affecting their life span

Anna Laitakari[1] | **Riikka Huttunen**[1] | **Paula Kuvaja**[2,3] | **Pauliina Hannuksela**[1] | **Zoltan Szabo**[4] | **Minna Heikkilä**[1] | **Risto Kerkelä**[4] | **Johanna Myllyharju**[1] | **Elitsa Y. Dimova**[1] | **Raisa Serpi**[1] | **Peppi Koivunen**[1]

[1]Biocenter Oulu, Faculty of Biochemistry and Molecular Medicine, Oulu Center for Cell-Matrix Research, University of Oulu, Oulu, Finland

[2]Cancer and Translational Medicine Research Unit, Medical Research Center Oulu, Oulu University Hospital, University of Oulu, Oulu, Finland

[3]Department of Pathology, Oulu University Hospital, Oulu, Finland

[4]Research Unit of Biomedicine, Department of Pharmacology and Toxicology, University of Oulu, Oulu, Finland

Correspondence
Peppi Koivunen, Biocenter Oulu, Faculty of Biochemistry and Molecular Medicine, Oulu Center for Cell-Matrix Research, University of Oulu, Aapistie 7C, Oulu FIN-90014, Finland.
Email: peppi.koivunen@oulu.fi

Funding information
Academy of Finland (Suomen Akatemia), Grant/Award Number: 266719, 308009, 296498 and 251314; Sigrid Juséliuksen Säätiö (Sigrid Jusélius Stiftelse); Finnish Cancer Foundation; Jane ja Aatos Erkon Säätiö (J&AE); FibroGen (FibroGen Inc.)

Abstract

Hypoxia inactivates hypoxia-inducible factor (HIF) prolyl 4-hydroxylases (HIF-P4Hs), which stabilize HIF and upregulate genes to restore tissue oxygenation. HIF-P4Hs can also be inhibited by small molecules studied in clinical trials for renal anemia. Knowledge of systemic long-term inactivation of HIF-P4Hs is limited but crucial, since HIF overexpression is associated with cancers. We aimed to determine the effects of systemic genetic inhibition of the most abundant isoenzyme HIF prolyl 4-hydroxylase-2 (HIF-P4H-2)/PHD2/EglN1 on life span and tissue homeostasis in aged mice. Our data showed no difference between wild-type and HIF-P4H-2-deficient mice in the average age reached. There were several differences, however, in the primary causes of death and comorbidities, the HIF-P4H-2-deficient mice having less inflammation, liver diseases, including cancer, and myocardial infarctions, and not developing anemia. No increased cancer incidence was observed due to HIF-P4H-2-deficiency. These data suggest that chronic inactivation of HIF-P4H-2 is not harmful but rather improves the quality of life in senescence.

KEYWORDS

anemia, HCC, hypoxia response, metabolism

Abbreviations: 2OG, 2-oxoglutarate; ALT, alanine aminotransferase; CCl_4, carbon tetrachloride; CKD, chronic kidney disease; COPD, chronic obstructive pulmonary disease; DEN, diethylnitrosamine; ECAR, extracellular acidification rate; EPO, erythropoietin; HCC, hepatocellular carcinoma; HIF, hypoxia-inducible factor; HIF-P4H-2, HIF prolyl 4-hydroxylase-2; HOMA-IR, homeostatic model assessment-insulin resistance; MEF, mouse embryonic fibroblast; OCR, oxygen consumption rate; OXPHOS, oxidative phosphorylation; PDK, pyruvate dehydrogenase kinase; pVHL, von Hippel Lindau protein; ROS, reactive oxygen species; VEGF, vascular endothelial growth factor.

1 | INTRODUCTION

Oxygen is vital for metazoan biological processes, and therefore a conserved rescue pathway for tackling hypoxia has evolved in all multicellular organisms from the simplest animal to human.[1-3] The central player in this pathway is the hypoxia-inducible factor (HIF), a dimeric transcription factor which upregulates the expression of several hundred genes to increase oxygen availability and delivery and to reduce its usage.[1] Thus HIF has a central role in inducing erythropoiesis and angiogenesis, and in reprogramming cellular energy metabolism to ensure ATP generation via non-oxygen-demanding pathways, for instance. Its target genes include, among others, erythropoietin (EPO), vascular endothelial growth factor (VEGF), numerous enzymes of glycolysis, and also pyruvate dehydrogenase kinase (PDK), which prevents the entry of pyruvate into the Krebs cycle and further to mitochondrial oxidative phosphorylation (OXPHOS).[4] HIF target genes also inhibit OXPHOS complex I activity and increase complex IV efficiency to reduce oxygen consumption and reduce the generation of detrimental reactive oxygen species (ROS).[5]

The stability of the HIFα subunits is regulated post-translationally by three HIF prolyl 4-hydroxylases (HIF-P4Hs, also known as PHDs or EglNs), which are enzymes that act as cellular oxygen sensors.[1] These require molecular oxygen, 2-oxoglutarate (2OG) and iron for the 4-hydroxylation of proline residues in HIFα, which earmarks it for proteasomal degradation via von Hippel Lindau protein (pVHL).[6] The HIF-P4Hs' affinity for oxygen is low, indicating that even a slight reduction in the oxygen concentration has a direct effect on the enzymes' catalytic activity.[7]

Small molecule HIF-P4H inhibitors, which are structural analogues of 2OG and stabilize HIFα in the presence of oxygen, are studied for the treatment of renal anemia due to their ability to induce EPO. Interestingly, in addition to increased hemoglobin levels, patients receiving them have been reported to have lowered serum total cholesterol levels, an improved HDL/LDL ratio and lower blood pressure.[8-11] Concerns about the safety of the long-term administration of HIF-P4H inhibitors have been raised since cancerous tumors typically express high levels of HIF, and HIF expression in cancers is often associated with increased mortality.[12] Although HIF stabilization in tumors results from intratumoral hypoxia, due to the cancer cell proliferation rate exceeding the vascularization rate, and HIF itself has not been proven oncogenic,[13] close care is required when administering HIF-P4H inhibitor therapy.

Aging is a natural phenomenon of all living organisms, eventually leading to pathologies and death. Many factors contribute to aging,[14] including telomere shortening, accumulation of ROS, genetic and epigenetic alterations, and aggregation of proteins leading to a senescent phenotype.[15] Aging is associated with metabolic changes such as increased obesity and declines in insulin secretion and sensitivity.[16] Obesity further predisposes to comorbidities such as cardiovascular disease, hepatic steatosis, and diabetes, so it is not surprising that longevity was first associated with calorie restriction.[17] Senescence is accompanied by chronic inflammation, and at the tissue level aging is characterized by increased fibrosis and tissue lipomatosis, that is, the replacement of functioning tissue by adipocytes.[18]

We have reported earlier that mice that are hypomorphic for HIF-P4H-2 (*Hif-p4h-2*$^{gt/gt}$), the most abundant HIF-P4H isoenzyme and the major one regulating HIFα stability, are protected from obesity, metabolic dysfunction, atherosclerosis, hepatic steatosis and cardiac and skeletal muscle ischemia.[19-24] As these mice do not develop the massive erythrocytosis associated with large-spectrum conditional inactivation of HIF-P4H-2, leading to premature death,[25,26] they offer a unique model for studying the consequences of its long-term inhibition at the organism level. They express less than 50% of wild-type (WT) *Hif-p4h-2* mRNA in most tissues and have normoxic stabilization of HIF1α/HIF2α in many tissues.[19,20] Based on the previous beneficial outcomes achieved with *Hif-p4h-2*$^{gt/gt}$ mice,[19-24] we set out to study whether the effects of chronic HIF-P4H-2 inhibition would influence the life span of the mice. We aged a cohort of male mice to senescence and determined their cause of death or the humane endpoint. In addition, we aged a cohort of female mice to 2 years of age to analyse aged tissues that were free of conditions causing death. Altogether, our data suggest that the long-term systemic inactivation of HIF-P4H-2 in mouse is safe. It did not alter the life span or result in increased cancer incidence, and the *Hif-p4h-2*$^{gt/gt}$ mice maintained the homeostasis in many tissues better than the WT.

2 | MATERIALS AND METHODS

2.1 | Animal experiments

All the animal experiments were performed according to protocols approved by the National Animal Experiment Board of Finland (license numbers ESAVI-6154 and ESAVI-8179). Power calculations were performed prior to the experiments in order to determine the smallest number of animals needed to obtain significant data. The *Hif-p4h-2*$^{gt/gt}$ mice were generated with a GeneTrap targeting vector introduced into intron 1 of the *Hif-p4h-2* gene, as previously described.[19] All the animals were fed a standard rodent diet *ad libitum* (18% kcal from fat, Teklad 2018, Envigo) and were housed in groups of 2-5 in the Laboratory Animal Center of the University of Oulu on a 12 hours light/dark cycle and at a constant temperature of 21-22°C, the males for as long as

possible until housed individually due to fighting or being the last one to survive. A male cohort of *Hif-p4h-2*$^{gt/gt}$ mice were allowed to age in their cages and their well-being was monitored 2-3 times per day on weekdays and once a day at weekends. Their body weight was measured once a month from 12 months old onwards. The mice were sacrificed when they reached a humane endpoint, and their organs were collected for analyses. If the mice were found dead during the night (total n = 5/53) and the cause of death could not be determined by postmortem necropsy, only the age at death was noted and the cause of death was recorded as unknown. The most likely causes of death or euthanasia and comorbidities were determined according to the recommended criteria.[27] The criteria for humane endpoints were a body weight loss of 20%, cold body temperature, pronounced inactivity or immobility, hunched posture with a matted or unkempt coat, a bleeding skin ulcer or rash, excessive abdominal swelling indicative of a tumor and increased respiratory effort. Age-matched groups were used for the analysis of tissues. A female cohort of *Hif-p4h-2*$^{gt/gt}$ mice was allowed to age to exactly 2 years and sacrificed. Gender and age-matched WT littermates were used as controls.

Hepatocellular carcinoma (HCC) was induced in the *Hif-p4h-2*$^{gt/gt}$ males and WT littermates by intraperitoneal (i.p.) injection of diethylnitrosamine (DEN, 25 mg/kg; N0258, Sigma-Aldrich; St. Louis, MO, USA) given at day 15 postpartum followed 2 weeks later by 6 weekly i.p. injections of carbon tetrachloride (CCl_4, 0.5 mL/kg; 289116, Sigma-Aldrich; St. Louis, MO, USA) dissolved in olive oil (O1514-100ML, Sigma-Aldrich; St. Louis, MO, USA). Tumor development was followed by ultrasound once a month from 4 months of age until sacrifice. The mice were sacrificed and their organs collected at the age of 9 months.

2.2 | Histological analyses

Five-micrometer sections were taken from formalin-fixed paraffin-embedded tissues, stained with H&E and viewed with a Leica DM LB2 or Olympus BX51 microscope and photographed with a Leica DFC 320 or Olympus DB71 camera. Brown adipose tissue (BAT) and skeletal muscle morphology were evaluated and the amounts of pancreatic lipomatosis and splenic megakaryocytes were scored (0 to 4). Hepatic steatosis, liver inflammation (neutrophils), and fibrosis were scored (0 to 4). Hepatocellular carcinomas were analyzed from H&E stained sections and the analyses confirmed from Gomori reticulum stained sections in a blinded fashion by an experienced pathologist (Dr. P. Kuvaja). Myocardial infarctions and fibrosis in the liver and lung were scored from Masson's Trichrome-stained tissue sections. Fibrosis in the kidney was quantified from five hot spots in 20× fields of Masson's Trichrome-stained tissue sections with Fiji (ImageJ).[28] The number and integrity of the kidney glomeruli were quantified from six 20× fields per mouse. Representative images of the gonadal white adipose tissue (WAT) (five 20× fields per mouse) were taken and the areas of 100 adipocytes were quantified with the Adobe Photoshop CS5 Magnetic Lasso Tool. Infiltration of CD68-positive macrophages into the WAT was quantified from immunohistochemical (IHC) stainings with an anti-CD68 antibody (ab955, Abcam; Cambridge, United Kingdom), measuring five 20× fields per sample. For the scoring of cancer incidence, one representative H&E-stained slide was evaluated for each tissue. Histological scoring was performed in a blinded fashion by an experienced mouse disease modeling pathologist (Dr. R. Serpi).

2.3 | Quantitative real-time PCR (qPCR) analyses

Total RNA was isolated from WAT, BAT, brain, and pancreas tissues with an E.Z.N.A. total RNA Kit II (Omega Bio-Tek; Norcross, GA, USA) and from cells and other tissues with TriPure Isolation Reagent (Roche Applied Science; Penzberg, Germany) and purified with the E.Z.N.A. total RNA Kit I (Omega Bio-Tek; Norcross, GA, USA), followed by reverse transcription with an iScript cDNA Synthesis Kit (Bio-Rad; Hercules, CA, United States). qPCR was performed with iTaq SYBR Green Supermix with ROX (Bio-Rad; Hercules, CA, United States) in a C1000 Touch Thermal Cycler and a CFX96 Touch Real-Time PCR Detection System (Bio-Rad; Hercules, CA, United States) with specific primers. Several primers used in this study were reported in our previous publications.[20,29] The new primer sequences of the specific primer pairs are listed in Table 1.

2.4 | Telomere length

Blood leukocyte total genomic DNA was extracted from the blood of 1-year-old male mice with the DNeasy Blood and Tissue Kit (69504, Qiagen). The telomere length was determined by a qPCR method developed for humans[30] and then modified for mice.[31] Primers for amplifying the telomeric region were used and the telomere length was calculated in relation to the single copy gene 36B4. Primer sequences are listed in Table 1.

2.5 | Blood and serum analyses

Serum was collected from the terminal blood of the mice at sacrifice. The blood glucose concentrations were determined with

TABLE 1 Primers used in the quantitative PCR analyses

Gene	Forward primer (5′→3′)	Reverse primer (5′→3′)
Acta2	GTCCCAGACATCAGGGAGTAA	TCGGATACTTCAGCGTCAGGA
Bgn	TGCCATGTGTCCTTTCGGTT	CAGGTCTAGCAGTGTGGTGTC
Cxcl2	CCCAGACAGAAGTCATAGCCAC	TGGTTCTTCCGTTGAGGGAC
Epo	CATCTGCGACAGTCGAGTTCTG	CACAACCCATCGTGACATTTT
Gsk3b	AAGCTCTGCGATTTTGGCAGT	GAGTTCTGGAGCACGGTAGTA
Hprt1	TCAGTCAACGGGGGACATAAA	GGGGCTGTACTGCTTAACCAG
Mmp12	TGCACTCTGCTGAAAGGAGTCT	GTCATTGGAATTCTGTCCTTTCCA
Ncf2	GCTGCGTGAACACTATCCTGG	AGGTCGTACTTCTCCATTCTGTA
Ppia	AGAACAATCCAGACTAGCAGCA	GGGAACTTCACATCACAGCTC
p16-Ink4a (*Cdkn2a*)	CCCAACGCCCCGAACT	GCAGAAGAGCTGCTACGTGAA
p21-Cip1 (*Cdkn1a*)	GCAGATCCACAGCGATATCCA	AACAGGTCGGACATCACCAG
Tgfb1	CACTGGAGTTGTACGGCAGTG	AGAGCAGTGAGCGCTGAATC
Tel-1b/ Tel-2b	CGGTTTGTTTGGGTTTGGGTTTGGGTTTGGGTTTGGGTT	GGCTTGCCTTACCCTTACCCTTACCCTTACCCTTACCCT
36B4	ACTGGTCTAGGACCCGAGAAG	TCAATGGTGCCTCTGGAGATT

a glucometer (Contour, Bayer; Leverkusen, Germany), the lactate levels with a lactometer (Lactate Scout+-meter, SensLab/EKF Diagnostics; Cardiff, United Kingdom) and the hemoglobin levels with a hemoglobin meter (HemoCue Hb 201+; Ängelholm, Sweden). Serum insulin and glucagon levels were determined with the Rat/Mouse Insulin ELISA kit (EZRMI-13K, Millipore) and Mouse Glucagon ELISA Kit (81518, CrystalChem). The homeostatic model assessment-insulin resistance (HOMA-IR) index was calculated from the blood glucose and serum insulin values. Serum total cholesterol, HDL cholesterol, triglyceride, and uric acid levels in the liver cancer cohort were determined by clinical analytical methods in Nordlab (Oulu University Hospital, Oulu, Finland). Serum total cholesterol, HDL cholesterol and triglyceride levels in the aged 2-year-old female cohort were determined by an enzymatic method (Roche Diagnostics), and LDL+VLDL cholesterol values were calculated using the Friedewald equation.[32] The ALT activity assay kit (MAK052, Sigma-Aldrich; St. Louis, MO, USA) was used to determine serum ALT levels and the Mouse Erythropoietin Quantikine ELISA kit (MEP00B, R&D Systems; Minneapolis, MN, USA) the EPO levels.

2.6 | Liver echography analyses

The development of liver tumors was followed using a high frequency linear array ultrasound platform (Vevo 2100, FUJIFILM VisualSonics, Inc.) with a microscan 550D transducer (40 MHz, 30 μm axial, 90 μm lateral resolution) under isoflurane-anesthesia on a heated examination table. The mice were subjected to the evaluation once a month from the age of 4 months until sacrifice.

2.7 | Determination of tissue glycogen

About 50 mg of liver or muscle was homogenized and the supernatant assayed with the Glycogen Assay Kit according to the manufacturer's instructions (700480, Cayman Chemical; Ann Arbor, MI, USA).

2.8 | Determination of hepatic triglycerides

Hepatic lipids were extracted by overnight digestion in an ethanol-KOH solution at +55°C and centrifuged. The lipids in the supernatant were precipitated on ice with $MgCl_2$ and the solution centrifuged again. The supernatant was assayed for triglycerides by an enzymatic method (Roche Diagnostics; Basel, Switzerland) and the absorbance of the colorimetric products was determined with the Infinite M1000 Pro Multimode Plate Reader (Tecan; Männedorf, Switzerland).

2.9 | Oxygen consumption and extracellular acidification rate measurements

Gender-matched mouse embryonic fibroblasts (MEFs) were isolated from *Hif-p4h-2*$^{gt/gt}$ and WT mice at E10.5 according to the protocol of[33] and immortalized. Real-time monitoring of oxygen consumption (OCR) and extracellular acidification (ECAR) rates was performed using a Seahorse XFp Analyzer, Seahorse XFp Cell Mito Stress Test Kit and Seahorse XFp Glycolysis Stress Test Kit (Agilent; Santa Clara, CA, United States) according to the manufacturer's protocols. Briefly, 1×10^4 MEFs were seeded in triplicate

onto XFp cell culture miniplates 6 hours in advance. The mitochondrial stress test was performed under basal conditions and in response to ATP synthase inhibitor oligomycin A (1 μM), mitochondrial uncoupler FCCP (2 μM), and the complex I and III inhibitors rotenone/antimycin A (0.5 μM) in Seahorse XF base medium supplemented with 10 mM glucose, 1 mM sodium pyruvate, and 2 mM L-glutamine. The glycolytic stress test was performed in response to glucose (10 mM), FCCP (2 μM), and 2-deoxyglucose (50 μM) in glucose-free medium supplemented with 2 mM L-glutamine. OCR is reported as pmol/min/10^4 cells and ECAR as mpH/min/10^4 cells. The calculations were performed with the Seahorse XF Report Generator software (Wave, Agilent). Basal respiration, basal glycolysis, glycolytic capacity, and glycolytic reserve were calculated according to the manufacturer's instructions.

2.10 | Western blot analyses

About 100 μg of total protein from lysed MEFs was resolved by SDS-PAGE, blotted, and probed with the following primary antibodies: HIF1α (NB100-479, Novus Biologicals), HIF-P4H-2 (NB100-2219, Novus Biologicals; Centennial, CO, USA), GLUT1 (NB300-666, Novus Biologicals; Centennial, CO, USA), PDK1 (KAP-PK112, Assay Designs; Ann Arbor, MI, USA), β-Actin (NB600-501, clone AC-15, Novus Biologicals; Centennial, CO, USA), and α-Tubulin (T-6199, Sigma-Aldrich; St. Louis, MO, USA) followed by a HRP-conjugated secondary antibody (1:5000; Bio-Rad; Hercules, CA, USA). The Pierce ECL system (ThermoScientific; Waltham, MA, USA) was used for detection.

2.11 | Statistics

Student's two-tailed *t* test was used for the statistical significances of differences between two groups and Fisher's exact test for data based on histological scoring. Areas under the curve were calculated by the summary measures method. All data are presented as means ± standard error of the mean (SEM), unless otherwise stated. $P < .05$ was considered statistically significant.

3 | RESULTS

3.1 | HIF-P4H-2-deficient mice maintain a lower body weight due to less adiposity throughout life and have no difference in life span relative to WT

The *ad libitum* normal chow-fed *Hif-p4h-2*$^{gt/gt}$ males and their WT littermates were allowed to age in their cages in the laboratory animal center. We followed the body weight of the mice until they were 26 months old (Figure 1A), after which the *n* was too small for statistical analyses. When the mice reached a humane endpoint, they were sacrificed and the organs were collected for analyses. The *Hif-p4h-2*$^{gt/gt}$ mice had about 20% lower body weight than the WT during the follow up (Figure 1A). At sacrifice their average body weight was 26.4 ± 1.2 g compared with 34.1 ± 1.6 g in the WT ($P = .0036$, Figure 1B). This weight difference resulted from a difference in adiposity, since the *Hif-p4h-2*$^{gt/gt}$ mice had >50% less WAT than the WT (Figure 1C). No significant difference in survival was observed between the genotypes (Figure 1D). The average ages at death for the WT and *Hif-p4h-2*$^{gt/gt}$ mice were 771 ± 22 days and 721 ± 28 days, respectively ($P = .19$, Figure 1E). Analyses of the telomere length in the 1-year-old WT and *Hif-p4h-2* leukocytes revealed no difference between the genotypes (Figure S1A), in agreement with the lack of any major difference in overall survival. Additionally, mRNA levels of the senescence markers *p16*^{Ink4a} (*Cdkn2a*), *p21*^{Cip1} (*Cdkn1a*), *Mmp12,* and *Cxcl2* were analyzed in selected tissues (Figure S1B), but no consistent differences in the senescence marker gene expression were observed in any tissue in the aged males nor in the 2-year-old female cohort (Figure S1B).

To ensure that the efficiency of the genetic knockdown by the gene trap had not been altered during aging, we analyzed the levels of WT *Hif-p4h-2* mRNA in the tissues at sacrifice, and found that the knockdown levels in the *Hif-p4h-2*$^{gt/gt}$ tissues had remained very similar, if not identical, to those analyzed in younger mice as reported by us earlier,[19,20,22] the heart having <10%, the skeletal muscle and BAT 20%, the kidney, spleen and lung 35%-45%, WAT and pancreas ~50%, and liver ~75% of the *Hif-p4h-2* mRNA to be found in the WT tissues (Figure 1F). Interestingly, the blood hemoglobin levels at sacrifice, although not erythrocytotic, were significantly higher in the *Hif-p4h-2*$^{gt/gt}$ mice than in the WT: 157 ± 8 g/L vs 124 ± 7 g/L ($P = .018$, Figure 1G). When compared to the hemoglobin levels of ~150 g/L reported earlier for both genotypes when 1 year old,[34] these data suggest that the *Hif-p4h-2*$^{gt/gt}$ mice were protected from the aging-associated anemia observed in the WT mice.

3.2 | HIF-P4H-2 deficiency protects against inflammation and liver disease, the most common causes of death in WT males

We next analyzed the causes of death or humane endpoints among the aged male mice according to the recommended criteria.[27] The initial cause was observed at autopsy and later verified by histological analyses. The most common cause of death or euthanasia in the aged WT males was inflammation,

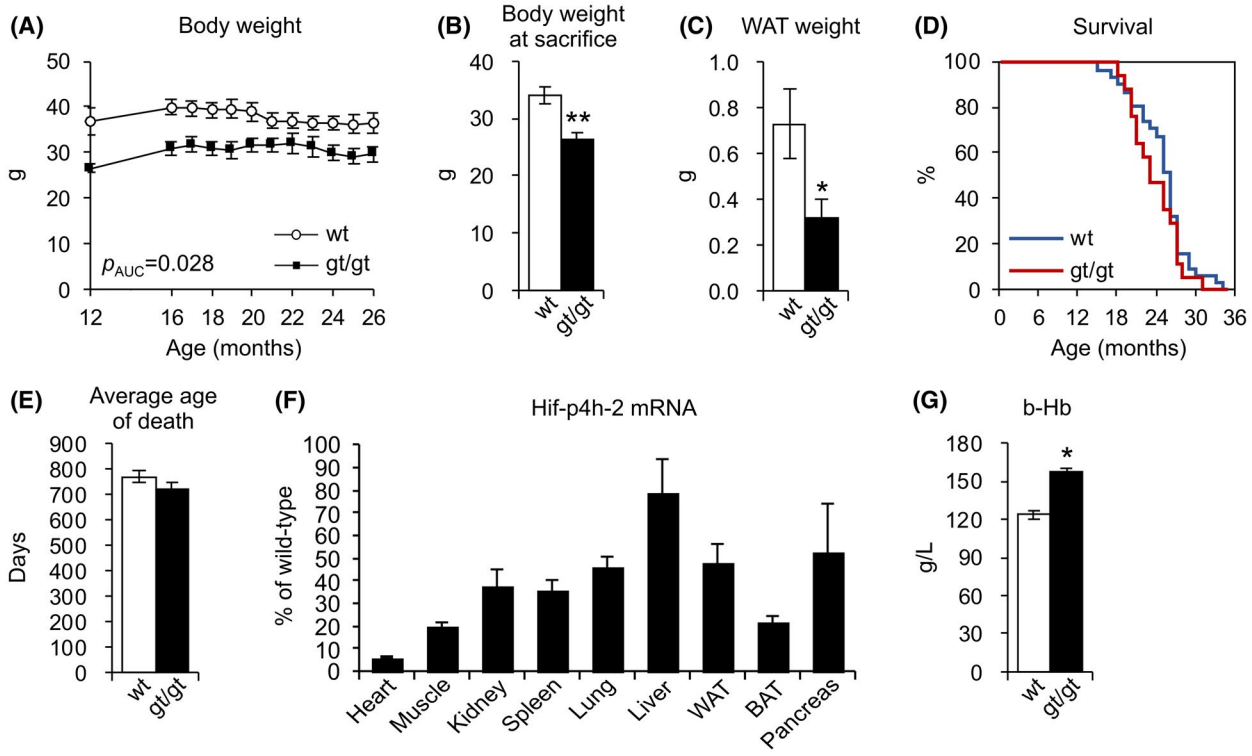

FIGURE 1 HIF-P4H-2-deficient (gt/gt) male mice are protected against obesity throughout life and have a similar life span to wild-type (WT) mice. A, Body weight development of 12-month-old wt and gt/gt mice up to 26 months of age (n = 6-25 wt, 4-15 gt/gt at different time points). B, Body weight at sacrifice (n = 30 wt, 14 gt/gt). C, Weight of gonadal WAT at sacrifice (n = 30 wt, 14 gt/gt). D, Kaplan-Meier survival analysis (n = 35 wt, 17 gt/gt). E, Average age at death (n = 35 wt, 17 gt/gt). F, *Hif-p4h-2* mRNA levels in gt/gt mice relative to wt. Gene expression was studied relative to peptidylprolyl isomerase A (*Ppia*) mRNA in kidney and pancreas and to β-actin mRNA in other tissues (n = 6/genotype). G, Blood hemoglobin levels (n = 12 wt, 4 gt/gt). Data are means ± SEM. (A-C, F-G) Age-matched cohorts were analyzed. *$P < .05$, **$P < .01$. The *P* value for (C) was calculated from log-transformed values. Abbreviations: b, blood; Hb, hemoglobin; WAT, white adipose tissue

accounting for 31% of the deaths, compared with 12% in the *Hif-p4h-2*$^{gt/gt}$ mice (Table 2). It appeared that a quarter of the WT mice died of a liver disease, which in 11% of the cases was steatohepatitis or hepatic fibrosis and in 14% HCC, while only 6% of the *Hif-p4h-2*$^{gt/gt}$ mice died of liver disease and none had HCC (Table 2). The genotypes had similar mortality due to gastrointestinal conditions and benign neoplasia, such as lipomas or hemangiomas (Table 2), while a humane endpoint for which no obvious cause was observed at autopsy was clearly more often reached in the *Hif-p4h-2*$^{gt/gt}$ mice than the WT (Table 2). The category of "others" included diagnoses such as hip dysfunction and breathing difficulties, each individual being affected by a different condition (Table 2). The most common comorbidity for both genotypes was myocardial infarction, which was nevertheless observed more in the WT mice (36%) than in the *Hif-p4h-2*$^{gt/gt}$ ones (21%) (Table 3). The second most common comorbidities in the WT mice were inflammation and seminal vesicle dilatation, which were observed in about a quarter of cases, while in the *Hif-p4h-2*$^{gt/gt}$ males they were found in only 11% and 6%, respectively (Table 3). In the *Hif-p4h-2*$^{gt/gt}$ mice the second most common comorbidity was steatohepatitis or hepatic fibrosis (Table 3), but it should be emphasized that liver diseases in the *Hif-p4h-2*$^{gt/gt}$ males very seldom reached the severity to be the primary cause of death (Table 2).

TABLE 2 Primary causes of death or euthanasia

Primary cause of death or euthanasia (%)	wt	gt/gt
Inflammation	30.6	11.8
Liver disease	25.0	5.9
Steatohepatitis or fibrosis	11.1	5.9
Hepatocellular carcinoma	13.9	0.0
Gastrointestinal condition	16.7	11.8
Benign neoplasia	8.3	11.8
Obesity	2.8	0.0
HEP reached	2.8	23.5
Others	2.8	11.8
Unknown	11.1	23.5
Total	100.0	100.0

N = 36 for wild-type (WT) and 17 for *Hif-p4h-2*$^{gt/gt}$(gt/gt).

Abbreviations: HEP, humane endpoint.

In view of the incidence of HCC as a common cause of death in WT mice, it was of importance to study the cancer incidence in other tissues. Thus the lung, spleen, kidney, pancreas, WAT, BAT, uterus (females), and testis (males) were analyzed. No tumors were found in most tissues, including the kidney, pancreas, testis, uterus, WAT, and BAT, while one WT female had a benign hemangioma in the spleen and one *Hif-p4h-2*$^{gt/gt}$ male a papillary adenocarcinoma in the lung, accounting for 14.3% and 9.1% of the mice, respectively (Table 4).

Since myocardial infarctions were common in both genotypes, we took a closer look at the hearts. Analyses of the male hearts revealed no difference in their weight between the genotypes: 231 ± 8 mg for the WT and 224 ± 12 mg for the *Hif-p4h-2*$^{gt/gt}$ (P = .63, Figure 2A). When age-matched cohorts were compared, small spontaneous, non-mortal cardiac infarcts were observed in 42% of the WT males but only 14% of their *Hif-p4h-2*$^{gt/g}$ counterparts (Figure 2B,C).

TABLE 3 Contributing causes (comorbidities)

Comorbidities (%)	wt	gt/gt
Myocardial infarction	35.7	21.4
Inflammation	25.8	11.8
Seminal vesicle dilation	22.6	5.9
Liver disease	9.7	17.6
Steatohepatitis or fibrosis	9.7	17.6
Benign neoplasia	9.7	5.9
Skin conditions	6.5	0.0
Gastrointestinal condition	3.2	0.0

The primary causes of death or euthanasia were excluded from the comorbidities.

N = 36 for wild-type (WT) and 17 for *Hif-p4h-2*$^{gt/gt}$ (gt/gt).

TABLE 4 Cancer incidence in indicated tissues (%)

	Males		Females	
Organ	wt	gt/gt	wt	gt/gt
Lung	0.0	9.1*	0.0	0.0
Spleen	0.0	0.0	14.3#	0.0
Kidney	0.0	0.0	0.0	0.0
Pancreas	0.0	0.0	0.0	0.0
Testis/uterus	0.0	0.0	0.0	0.0
White adipose tissue	0.0	0.0	0.0	0.0
Brown adipose tissue	0.0	0.0	0.0	0.0

Wild-type(wt) and *Hif-p4h-2*$^{gt/gt}$ (gt/gt) mice. N = 7-29 for males and 7/genotype for females.

Tumor type: *Papillary adenocarcinoma, #Benign hemangioma.

3.3 | Systemic long-term HIF-P4H-2 inhibition protects male mice from hepatic inflammation, fibrosis and cancer

When the liver weights were analyzed at sacrifice, a significant difference was observed in favor of the *Hif-p4h-2*$^{gt/gt}$ males: 1.923 ± 0.202 g for WT vs. 1.236 ± 0.077 g for *Hif-p4h-2*$^{gt/gt}$ (P = .026, Figure 3A). About 30% of both genotypes had steatosis, which was moderate in 15% of the WT livers and mild in 15%, while only mild steatosis was observed in the *Hif-p4h-2*$^{gt/gt}$ livers (Figure 3B). Sixty percentage of the WT livers had inflammation, which was severe in 20% of the cases, while only 25% of the *Hif-p4h-2*$^{gt/gt}$ livers had inflammation and in all cases it was classified as moderate (P =.079) (Figure 3C). Over 50% of the WT livers had fibrosis, while this was observed in only <10% of the *Hif-p4h-2*$^{gt/gt}$ livers (P = .01, Figure 3D). Interestingly, 20% of the WT males had developed spontaneous HCC compared to none of the *Hif-p4h-2*$^{gt/gt}$ mice (P = .14) when age-matched cohorts were compared. These data together with our earlier findings in 1-year-old male mice[20] suggest that non-alcoholic fatty liver disease characterized by steatosis had advanced to steatohepatitis, fibrosis and even HCC in the aged WT males, while the HIF-P4H-2 deficiency had provided protection from this disease.

3.4 | HIF-P4H-2-deficient mice retain a healthier metabolism and develop less carcinomas in a chemically induced HCC model

Encouraged by the above data, we subjected the *Hif-p4h-2*$^{gt/gt}$ and WT males to a DEN and CCl_4 chemical-induced model of HCC. The genotoxic carcinogen DEN was administered to 2-week-old mice followed by a once a week dose of the fibrotic promoter CCl_4 starting at the age of 4 weeks and continuing for 6 weeks. We then followed the development of tumors by means of ultrasound scans starting 4 months after the DEN injection and continuing until the mice were sacrificed at 9 months of age, the time of the sacrifice being based on the ultrasound scan results (Figure S2). At this point, consistent with our previous data, the body weight of the *Hif-p4h-2*$^{gt/gt}$ mice was ~20% lower than that of the WT (Figure 4A) and they had about 50% less WAT (Figure 4B). Moreover, their livers were 20% lighter (Figure 4C), whereas serum ALT levels were pathologically increased (above 55 IU/L that is usually regarded as the physiological limit) in all the mice, with no difference between the genotypes (Figure 4D). The *Hif-p4h-2*$^{gt/gt}$ mice had slightly lower serum cholesterol and HDL cholesterol levels, but the difference did not reach significance, while no differences were observed in the serum triglyceride levels (Figure 4E-G). Moreover, the serum levels of uric acid, a marker of chronic inflammation

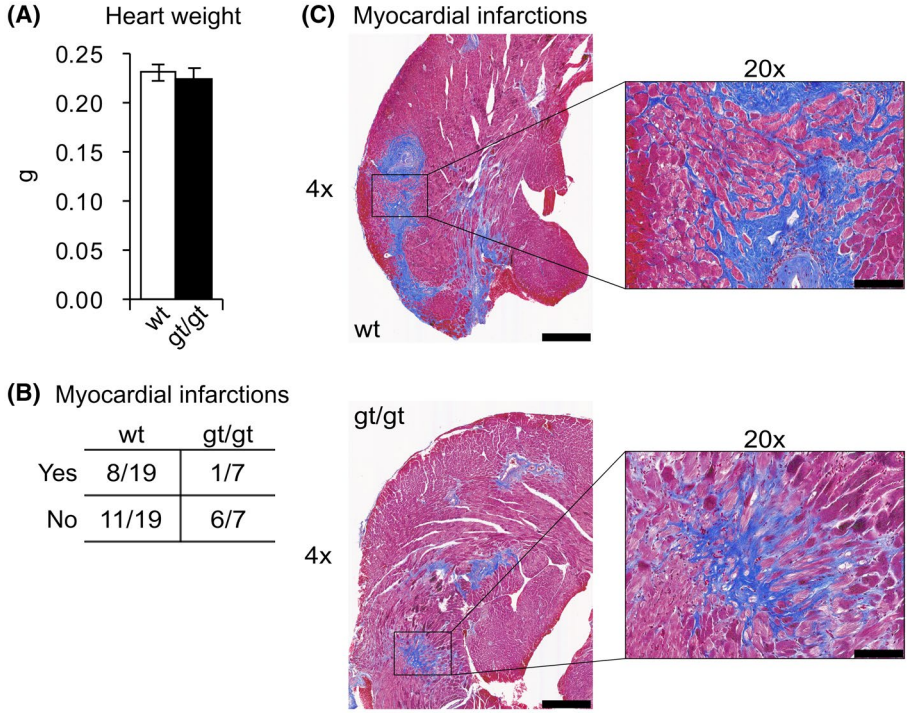

(B) Myocardial infarctions

	wt	gt/gt
Yes	8/19	1/7
No	11/19	6/7

FIGURE 2 Aged wild-type (WT) male mice have more spontaneous myocardial infarcts than HIF-P4H-2-deficient (gt/gt) mice. A, Heart weight at sacrifice (n = 30 wt, 14 gt/gt). B, Myocardial infarctions analyzed from (C) Masson's trichrome-stained heart sections (n = 19 wt, 7 gt/gt). Data for (A) are means ± SEM. Age-matched cohorts were analyzed. Scale bar = 500 μm for 4× and 100 μm for 20×

which has been associated with all-cause and cardiovascular mortality and with an increased risk of cancer in humans,[35-37] were significantly lower in the *Hif-p4h-2*$^{gt/gt}$ mice than in the WT group (Figure 4H), and their blood lactate/glucose ratio was lower (Figure 4I). Interestingly, histological analyses of the livers showed that only 33% of the *Hif-p4h-2*$^{gt/gt}$ mice had developed HCC compared with 69% of the WT (P = .12) (Figure 4J,K). There was no difference in tumor size between the genotypes. Of the mice that did not develop HCC, the majority showed varying levels of hepatic regeneration or degeneration as a response to the carcinogenic stimulus, and no difference in the prevalence of these was observed between the genotypes. Altogether, these data suggest that the better-preserved liver and metabolic health of the *Hif-p4h-2*$^{gt/gt}$ mice ameliorated the chemically induced carcinogenesis, and that chronic stabilization of HIFα due to HIF-P4H-2 deficiency did not exacerbate HCC.

3.5 | Protection from aging-associated obesity and adiposity in the HIF-P4H-2-deficient mice is independent of gender and associated with improved tissue homeostasis in the liver, muscle, and pancreas

To study aged tissues that are free of disease and other conditions leading to death, and also the potential dependence of the previous findings on gender, we next aged a female mouse cohort to exactly 2 years of age and analyzed their tissues at sacrifice. The *Hif-p4h-2*$^{gt/gt}$ mice weighed significantly less than the WT mice and had less WAT and WAT inflammation, while the reduced size of the adipocytes did not reach significance (Figure 5A-D). There was no difference in the amount or morphology of the BAT between the genotypes (Figure 5E,F), nor were any significant differences between the genotypes detected either in the serum cholesterol and lipids, or in blood glucose, serum insulin, HOMA-IR or serum glucagon levels (Figure S3). Samples were not taken in a fasted state because of the advanced age of the mice, which could have caused a difference relative to the previously reported healthier values for fasted *Hif-p4h-2*$^{gt/gt}$ mice.[20] As in the males (Figure 1F), the knockdown levels of *Hif-p4h-2* mRNA in the tissues of the aged females (Figure 5G) had remained very similar, if not identical, to levels reported in younger mice.[19,20,22]

No difference in the weight of the heart (Figure 6A) or in the histological findings (Figure 6B) were observed between the genotypes, the hearts of the 2-year-old females thus being healthier than those of the aged males (Figure 2B, average age of age-matched cohorts 2.0-years). There were also no obvious differences in the histology of the female skeletal muscle between the genotypes (Figure 6C), but the *Hif-p4h-2*$^{gt/gt}$ muscles had a >40% higher glycogen content than the WT ones (Figure 6D), which was in agreement

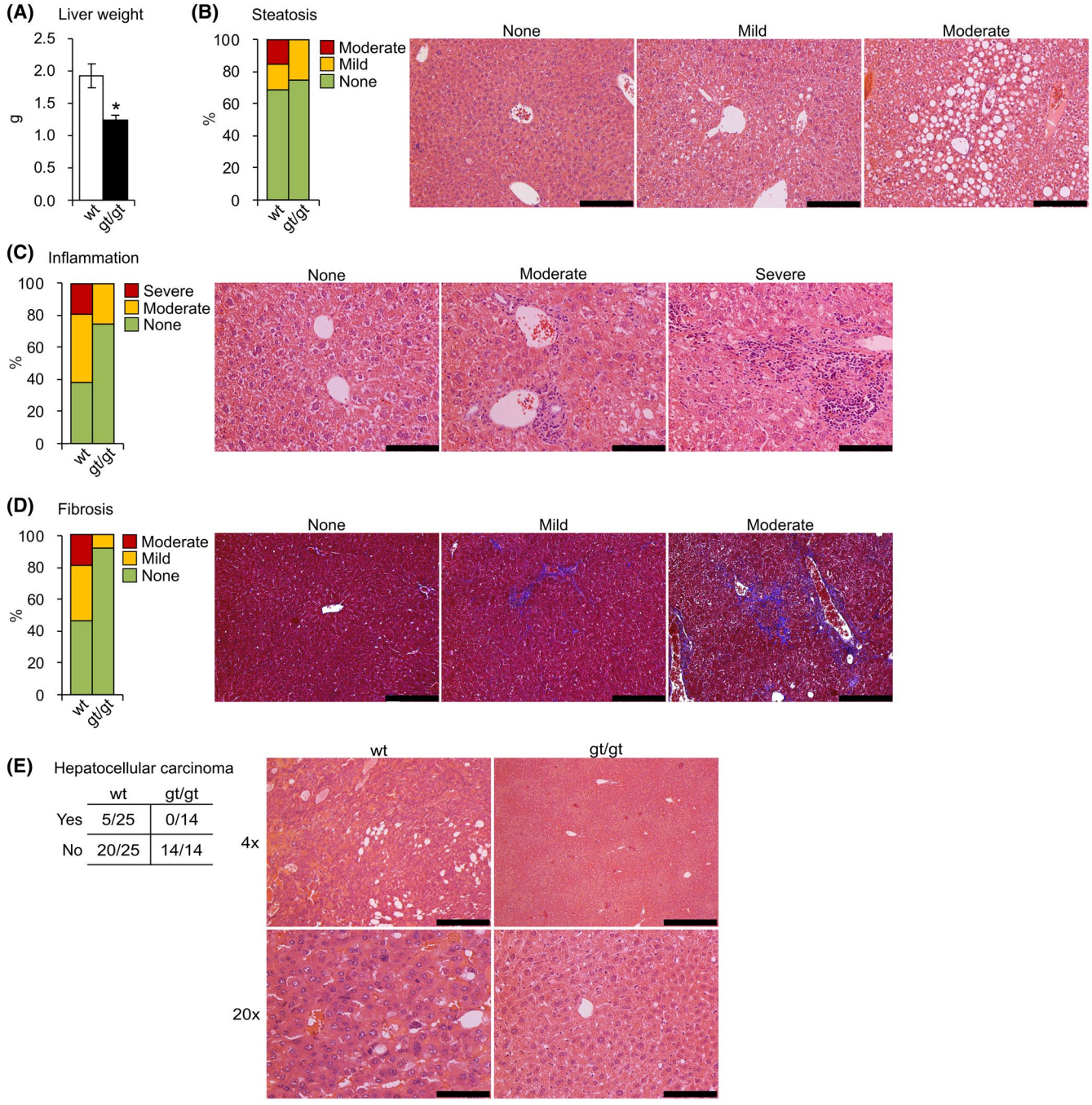

FIGURE 3 Aged HIF-P4H-2-deficient (gt/gt) male mice are protected against age-induced liver disease and hepatocellular carcinoma as compared with wild-type (WT) mice. A, Liver weight (n = 30 wt, 14 gt/gt). B, Scoring of steatosis from H&E-stained liver sections. Grading: "None" corresponds to score 0, "Mild" to 1 and "Moderate" to 2-3. C, Scoring of inflammation (neutrophils) from H&E-stained liver sections. Grading: "None" corresponds to score 0, "Moderate" to 1-2 and "Severe" to 3-4. D, Scoring of fibrosis from Masson's trichrome-stained liver sections. Grading: "None" corresponds to score 0, "Mild" to 1 and "Moderate" to 2. E, Hepatocellular carcinomas from H&E-stained sections. Data in (A) are means ± SEM. Age-matched cohorts were analyzed. (B-E) n = 26 wt, 12 gt/gt, images are representative of scoring for wt. Scale bars: (B-D) 200 μm, (C) 100 μm, (E) 500 μm for 4× and 100 μm for 20×. $*P < .05$

with their increased expression of glycogen branching enzyme 1 (*Gbe1*) and glycogenin (*Gyg1*) mRNAs (Figure 6E).

The livers of the *Hif-p4h-2*$^{gt/gt}$ females were about 25% lighter than those of the WT (Figure 7A). Histological analyses of steatosis, inflammation and fibrosis revealed very low levels of these in all the mice, with no difference between the genotypes (Figure 7B-D). The liver triglyceride concentrations were in line with this, the levels being relatively low in all the mice, again with no difference between the genotypes (Figure 7E). In contrast, the liver glycogen content in the WT females was significantly, about two-fold, higher than that in their

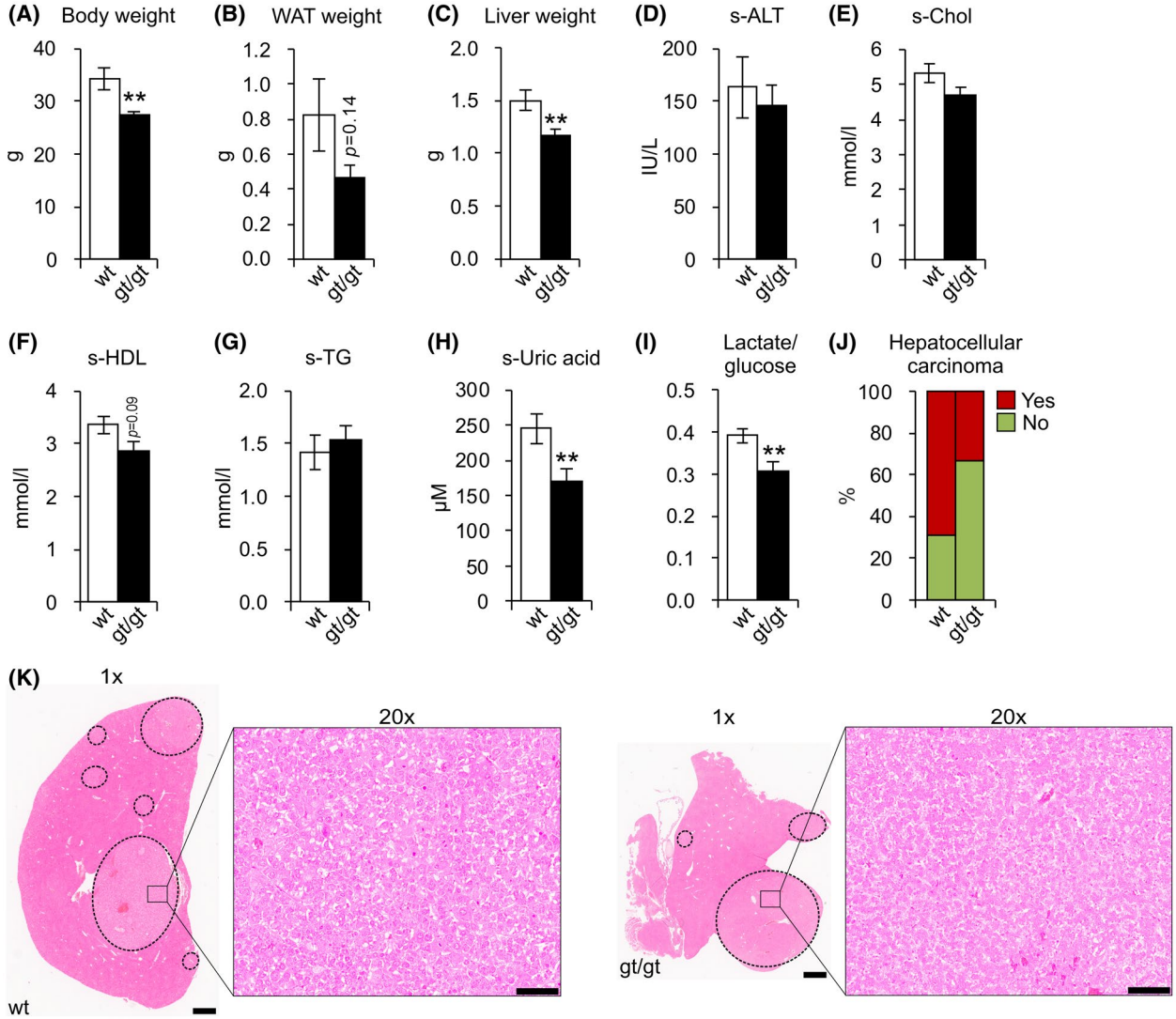

FIGURE 4 Fewer HIF-P4H-2-deficient (gt/gt) male mice develop chemically induced liver cancer than wild-type (WT) mice. (A) Body weight at sacrifice. (B) Weight of gonadal WAT. (C) Liver weight. (D) Serum ALT levels. (E) Serum total cholesterol, (F) HDL cholesterol and (G) triglyceride levels. (H) Serum uric acid levels. (I) Blood lactate-to-glucose ratio. (J) Hepatocellular carcinomas analyzed from (K) H&E-stained tissue sections. Data are means ± SEM. n = 13 wt, 12 gt/gt. Scale bar = 1 mm for 1× and 100 µm for 20×. $^{**}P < .01$. Abbreviations: ALT, alanine aminotransferase; s, serum; TG, triglyceride; WAT, white adipose tissue

Hif-p4h-2$^{gt/gt}$ counterparts (Figure 7F), this being in agreement with the overall better metabolic health of the latter, which results in less glucose being stored in their liver. In line with the overall healthier state of the female livers compared with those of the males, no HCC was observed in any of the female livers.

Interestingly, the pancreas histology showed significantly more lipomatosis in the aged WT mice than in the *Hif-p4h-2*$^{gt/gt}$ group (Figure 7G), suggesting that HIF-P4H-2 deficiency also provides protection for the pancreas and being in agreement with the lower adiposity of the *Hif-p4h-2*$^{gt/gt}$ females (Figure 5A,B).

The histological analyses of the female lungs showed no differences in the overall architecture or in the amount of fibrosis (Figure 8). This is of importance since in earlier studies HIF-P4H-2 deficiency present only in endothelial and hematopoietic cells has been associated with increased pulmonary arterial hypertension,[38] and with an increased prevalence of chronic obstructive pulmonary disease (COPD).[39]

3.6 | Chronic HIF-P4H-2 deficiency provides protection against aging-associated kidney disease and anemia

No difference in the number of kidney glomeruli was seen between the 2-year-old WT and *Hif-p4h-2*$^{gt/gt}$ females in the histological analyses (Figure 9A), but the number of shrunken

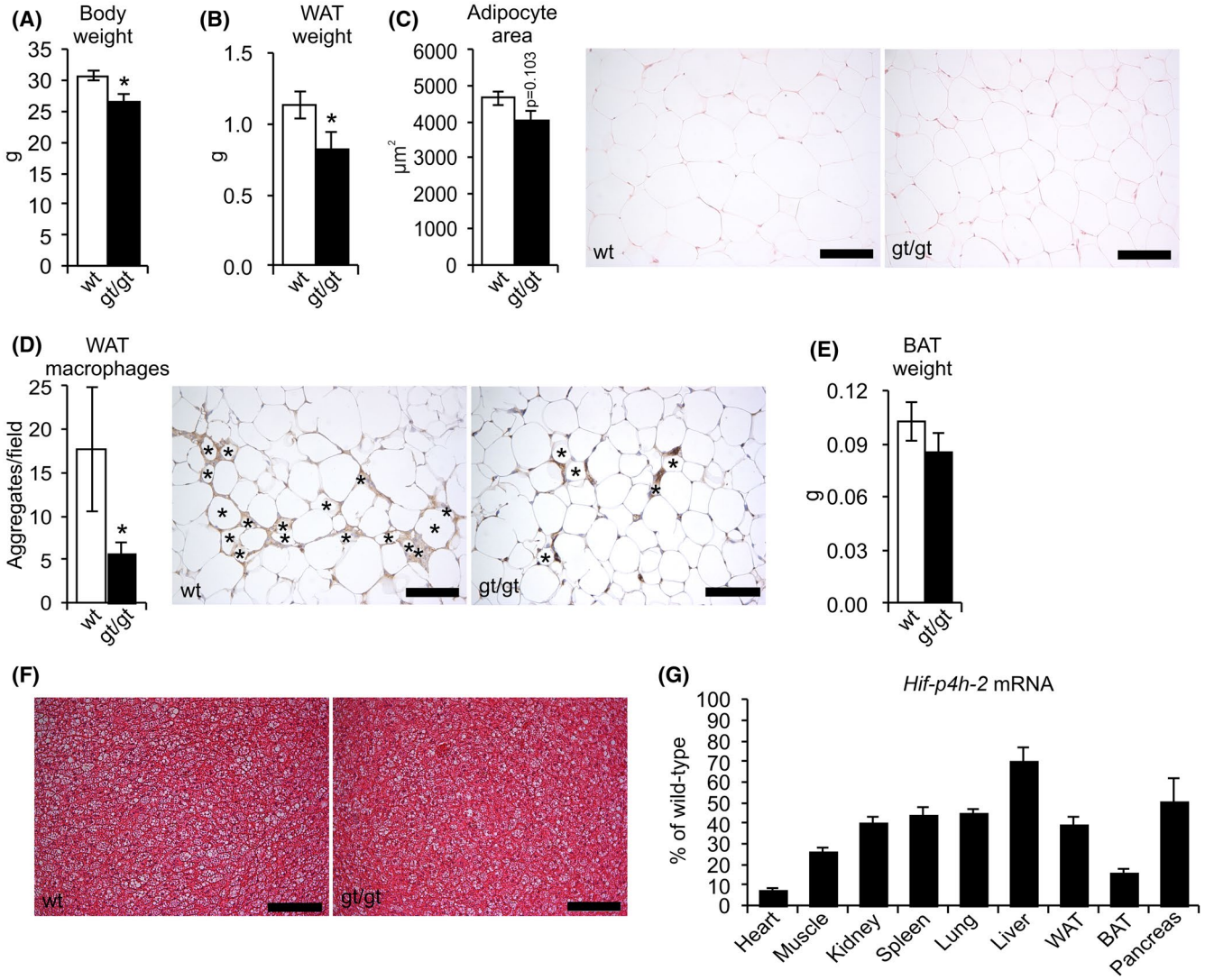

FIGURE 5 HIF-P4H-2-deficient (gt/gt) female mice maintain lower body weight, WAT weight and have less WAT inflammation than wild-type (WT) mice at 2 years of age. A, Body weight at sacrifice. B, Weight of gonadal WAT. C, Cross-sectional area of WAT adipocytes. D, Number of macrophage aggregates in WAT. (*) = Adipocytes surrounded by macrophage aggregates. E, BAT weight. F, BAT morphology from H&E-stained sections. G, *Hif-p4h-2* mRNA levels in gt/gt mice relative to wt. Gene expression was studied relative to peptidylprolyl isomerase A (*Ppia*) mRNA in kidney and pancreas and to β-actin mRNA in other tissues. Data are means ± SEM. n = 7/genotype. Scale bars = 100 μm. $*P < .05$. Abbreviations: BAT, brown adipose tissue; WAT, white adipose tissue

glomeruli was 4.5 times higher in the former (Figure 9B). Additionally, the amount of interstitial renal fibrosis in the WT kidneys was more than double that in the *Hif-p4h-2*$^{gt/gt}$ ones, and it was associated with significantly reduced levels of renal fibrotic mRNAs, transforming growth factor beta 1 (*Tgfb1*), smooth muscle actin alpha 2 (*Acta2*), neutrophil cytosolic factor 2 (*Ncf2*), and biglycan (*Bgn*), in the latter (Figure 9C,D).

Chronic kidney disease (CKD) is characterized by damaged glomeruli and tubuli and results in anemia due to EPO being produced mostly by the kidney. Obesity, diabetes, and high blood pressure entail a predisposition to CKD. In this case the blood hemoglobin levels of the aged females were 126 ± 3 g/L for the WT mice and 162 ± 6 g/L for the *Hif-p4h-2*$^{gt/gt}$ mice ($P = 8.8 \times 10^{-5}$, Figure 9E), indicating that the aged WT mice of both genders were anemic (Figure 1G). We next analyzed serum EPO levels and found them to be significantly, ~40%, higher in the *Hif-p4h-2*$^{gt/gt}$ females than in the WT group (Figure 9F), whereas only a trend toward higher renal *Epo* mRNA level was detected (Figure 9D).

We have reported earlier that *Hif-p4h-2*$^{gt/gt}$ mice develop slight erythrocytosis.[34] This appeared to result from an increased differentiation of splenic hematopoietic stem cells, resulting in splenomegaly due to upregulation of HIF2α and the concomitant downregulation of Notch signaling in the spleen.[34] Unlike the situation in these 1-year-old mice, no difference in spleen weight was observed here between the genotypes at 2 years of age (Figure 9G). Histological analyses of the spleens showed no major alterations in the

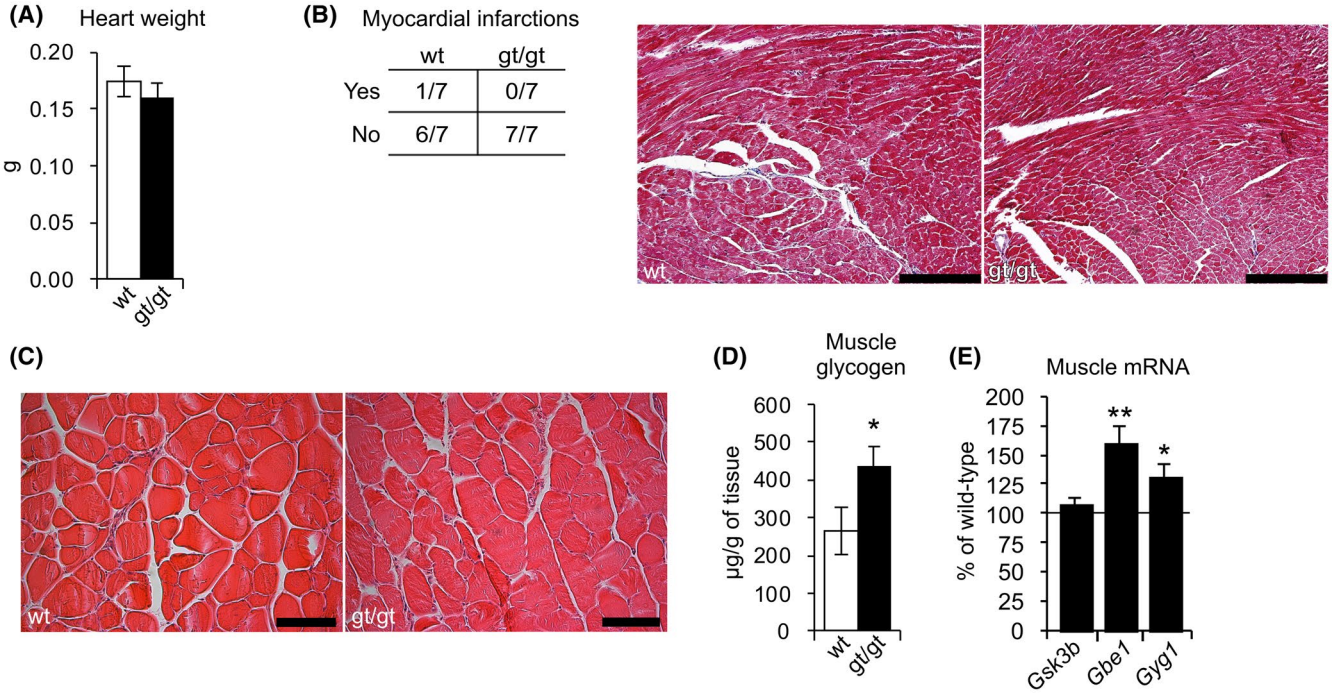

FIGURE 6 Two-year-old HIF-P4H-2-deficient (gt/gt) female mice have similar heart health to wild-type (WT) mice but more glycogen in their skeletal muscle. A, Heart weight at sacrifice. B, Myocardial infarctions analyzed from Masson's trichrome-stained heart sections. C, Skeletal muscle morphology from H&E-stained sections. D, Muscle glycogen content. E, mRNA levels in the skeletal muscle of gt/gt mice relative to wt. Gene expression was studied relative to hypoxanthine phosphoribosyltransferase 1 (*Hprt1*) mRNA. Data are means ± SEM. n = 7/genotype. Scale bars: (B) 200 µm, (C) 100 µm. $*P < .05$, $**P < .01$. Abbreviations: Gbe1, 1,4-alpha-glucan branching enzyme 1; Gsk3b, glycogen synthase kinase 3 beta; Gyg1, glycogenin 1

overall architecture between the genotypes, while slightly more megakaryocytes and erythroid hyperplasia were detected in the *Hif-p4h-2*$^{gt/gt}$ spleens than in the WT ones (Figure 9H). Altogether, these data suggest that, in addition to the splenic extramedullary erythrocytosis seen in the *Hif-p4h-2*$^{gt/gt}$ mice, the ability of these mice to retain normal hemoglobin levels at a very advanced age results from better preserved renal homeostasis.

3.7 | HIF-P4H-2-deficient MEFs show increased glycolysis and decreased oxygen consumption and ATP production

To deepen our understanding of the molecular mechanisms behind the metabolic differences observed here and reported earlier,[19-24] we isolated MEFs from the *Hif-p4h-2*$^{gt/gt}$ and WT mice at E10.5. The *Hif-p4h-2* mRNA levels in the *Hif-p4h-2*$^{gt/gt}$ MEFs were 17% of those in the WT (Figure 10A) and they had stabilization of HIF1α (Figure 10B) under normoxia but not of HIF2α (data not shown). Of the metabolic HIF target genes studied, upregulation of the mRNA levels of glucose transporter 4 (*Glut4*), phosphofructokinase L (*Pfkl*), and pyruvate dehydrogenase kinase 1 (*Pdk1*) was seen in the *Hif-p4h-2*$^{gt/gt}$ MEFs compared with the WT (Figure 10A). Protein levels of GLUT1 and PDK1 were upregulated in the former (Figure 10B). We next subjected the MEFs to analyses of real-time changes in the mitochondrial oxygen consumption rate (OCR) and the extracellular acidification rate (ECAR), which are reflective of oxidative metabolism and glycolysis, respectively, at the baseline and following mitochondrial and glycolytic stress tests. The baseline and stressed OCR values were significantly, ~50%, lower in the *Hif-p4h-2*$^{gt/gt}$ MEFs than in the WT (Figure 10C). ATP production in the *Hif-p4h-2*$^{gt/gt}$ MEFs was half of that in the WT and their proton leak was 65% of that in the WT (Figure 10C). In response to the glycolytic stress test the *Hif-p4h-2*$^{gt/gt}$ MEFs manifested increased ECAR relative to the WT cells, showing significantly elevated glycolysis (143%), glycolytic capacity (127%) and glycolytic reserve (160%) (Figure 10D). Altogether, the data presented here associate the HIF-mediated upregulation of the key glycolytic mRNAs in the *Hif-p4h-2*$^{gt/gt}$ MEFs (Figure 10A), as also shown earlier in *Hif-p4h-2*$^{gt/gt}$ mice,[20] with decreased energy production, which in turn is probably associated with the protection against obesity and adiposity and the overall better metabolic health observed in the *Hif-p4h-2*$^{gt/gt}$ mice.

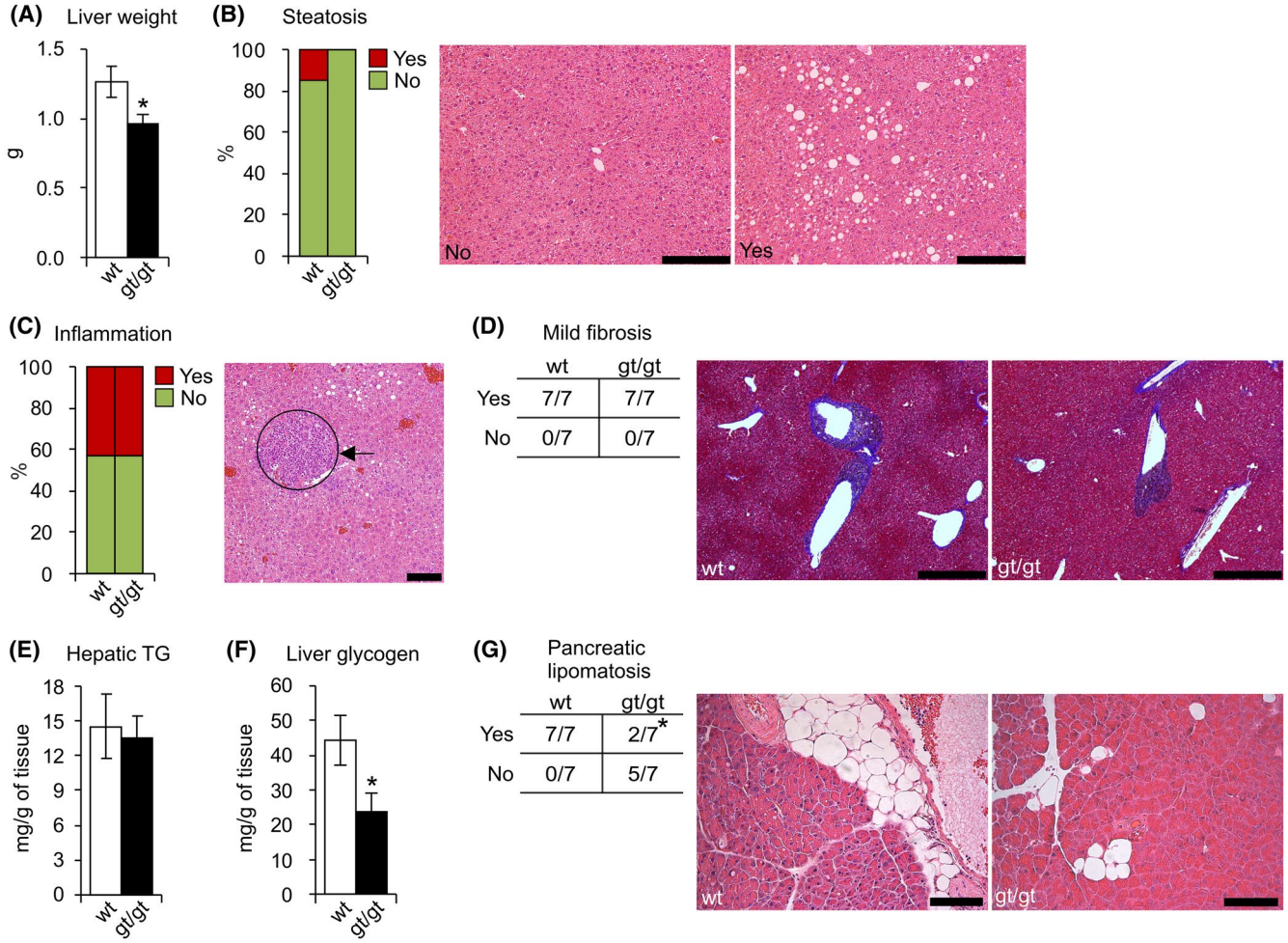

FIGURE 7 Two-year-old HIF-P4H-2-deficient (gt/gt) female mice have similar liver health to wild-type (WT) mice, but lower liver glycogen content and less pancreatic lipomatosis. A, Liver weight at sacrifice. B, Scoring of steatosis from H&E-stained liver sections. Grading: "No" corresponds to score 0-1 and "Yes" to 2. C, Scoring of inflammation from H&E-stained liver sections. Grading: "No" corresponds to score 0-1 and "Yes" to 2-3. Arrow indicates neutrophil clusters. D, Scoring of fibrosis from Masson's trichrome-stained liver sections. "Mild fibrosis" corresponds to scores 1-2. E, Hepatic triglyceride content. F, Liver glycogen content. G, Pancreatic lipomatosis from H&E-stained sections. Data for A, E, F are means ± SEM. n = 7/genotype. (B, C) Images are representative of scoring for wt. Scale bars: (B, D) 200 μm, (C, G) 100 μm. *$P < .05$. Abbreviations: TG, triglyceride

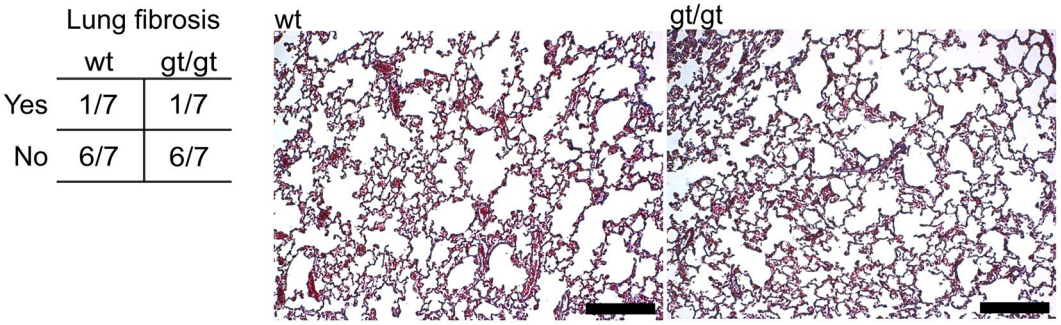

FIGURE 8 Lungs of 2-year-old HIF-P4H-2-deficient (gt/gt) and wild-type (WT) female mice have similar morphology and level of fibrosis. Analysis of lung fibrosis from Masson's trichrome-stained sections. n = 7/genotype. Scale bar = 200 μm

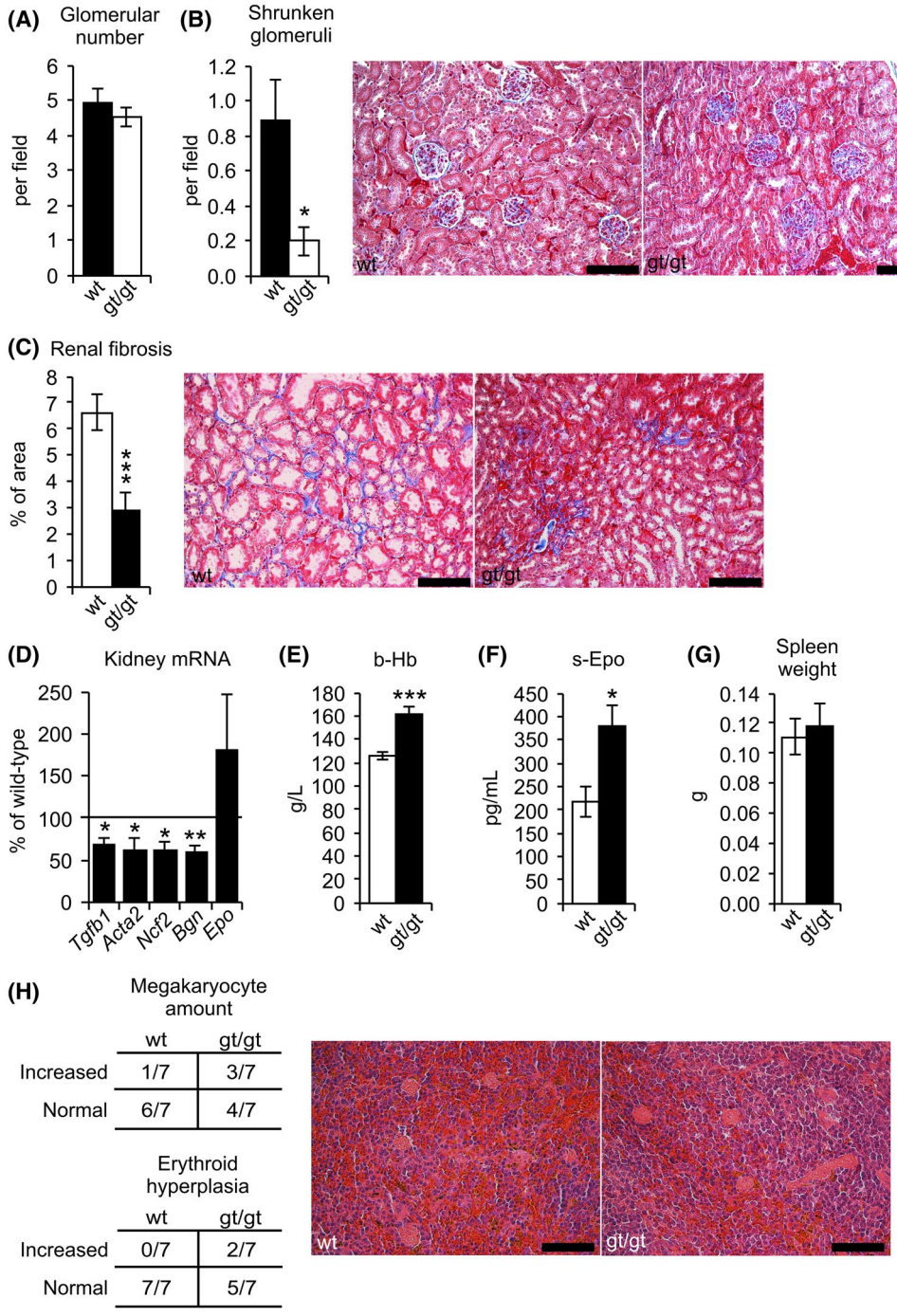

FIGURE 9 Two-year-old HIF-P4H-2-deficient (gt/gt) female mice have healthier kidney morphology and are protected against age-induced anemia relative to wild-type (WT) mice. (A) Kidney glomerular number and (B) glomerular integrity, as the number of shrunken glomeruli per 20× field in H&E-stained sections. (C) Area of renal fibrosis per 20× field in Masson's trichrome-stained sections. (D) mRNA levels in the kidney of gt/gt mice relative to wt. Gene expression was studied relative to peptidylprolyl isomerase A (*Ppia*) mRNA. (E) Blood hemoglobin levels. (F) Serum erythropoietin levels. (G) Spleen weight. (H) Megakaryocyte amount and erythroid hyperplasia in H&E-stained spleen sections. Data in A-G are means ± SEM. n = 7/genotype. Scale bars: (B, C) 100 µm, (H) 50 µm. *$P < .05$, **$P < .01$, ***$P < .001$. Abbreviations: Acta2, actin alpha 2; b, blood; Bgn, biglycan; EPO, erythropoietin; Hb, hemoglobin; Ncf2, neutrophil cytosolic factor 2; s, serum; Tgfb1, transforming growth factor beta 1

4 | DISCUSSION

Ever since the 1800s, mountain sanatoriums at high altitudes have been places for treating illness and other harmful conditions, especially tuberculosis in the pre-antibiotic era. Exposure to high altitudes has also been studied for the treatment of cardiac ischemia, dyslipoproteinemia and hypertension,[40-42] and similarly endurance athletes have been

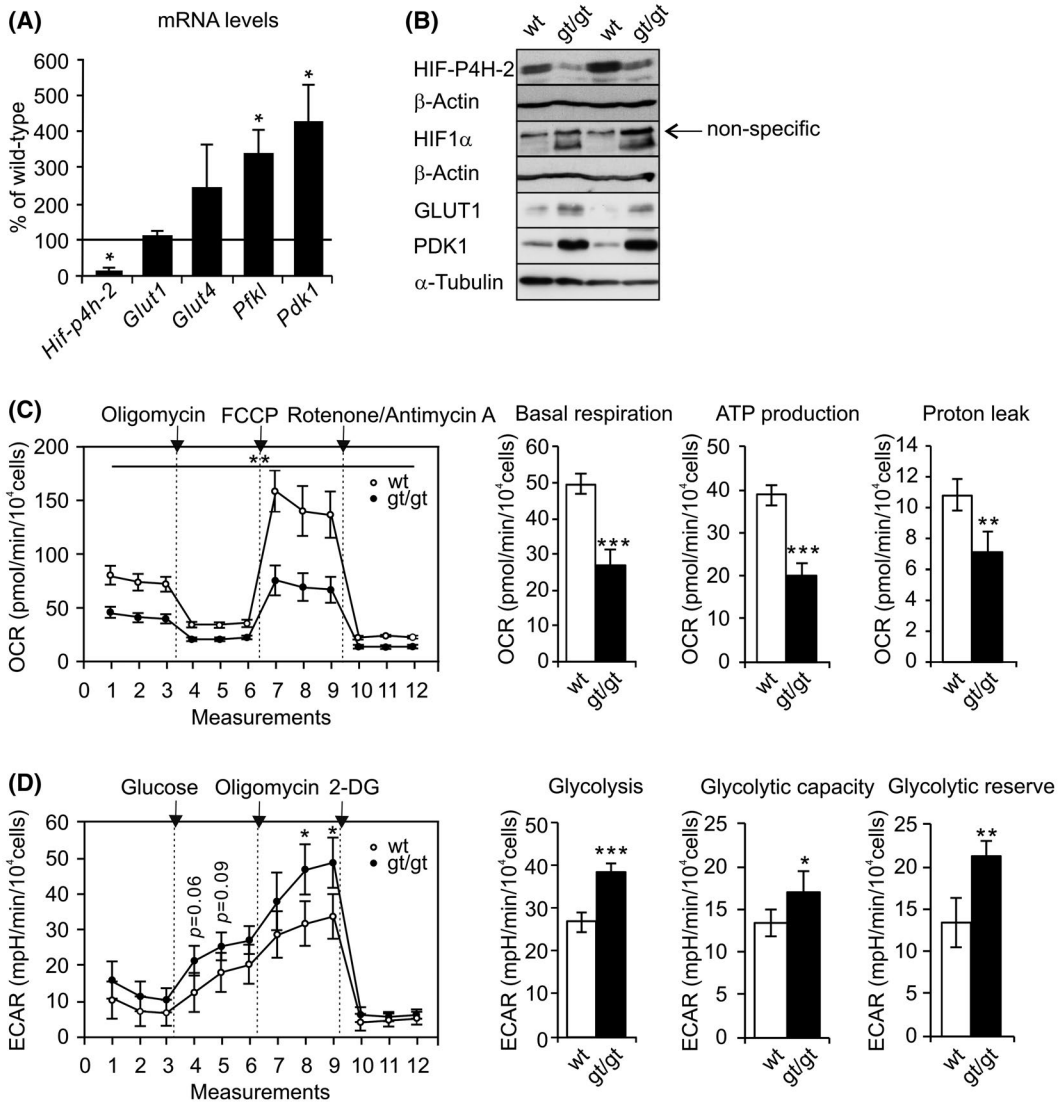

FIGURE 10 Metabolic reprogramming in the HIF-P4H-2-deficient mouse embryonic fibroblasts (MEFs). A, mRNA levels of gt/gt MEFs relative to wild-type (WT), studied relative to TATA-box binding protein mRNA (n = 3 wt, 4 gt/gt). B, Representative Western blot analyses of HIF-P4H-2, HIF1α, GLUT1, and PDK1 protein levels. β-actin and α-tubulin were used as loading controls. C, Oxygen consumption rate (OCR) profile plot and quantification of basal respiration, ATP-linked respiration as ATP production and proton leak (n = 3 wt, 4 gt/gt). OCR was analyzed under basal conditions and in response to treatments (indicated by arrows) with oligomycin, FCCP and rotenone-antimycin A, 3 measurements/each. D, Extracellular acidification rate (ECAR) profile plot and quantification of glycolysis, glycolytic capacity, and glycolytic reserve (n = 3 wt, 3 gt/gt). Kinetic ECAR response to treatments (indicated by arrows) with glucose, oligomycin and 2-deoxyglucose, 3 measurements/each. Data are means ± SEM. *$P < .05$, **$P < .01$, ***$P < .001$. Abbreviations: 2-DG, 2-deoxyglucose; FCCP, carbonyl cyanide-4-(trifluoromethoxy) phenylhydrazone; GLUT, glucose transporter; PDK1, pyruvate dehydrogenase 1; PFKL, phosphofructokinase, liver type

exploiting high altitude training for several decades.[43] Our knowledge of the long-term consequences of activation of the hypoxia response pathway relies mostly on data reported from people exposed to environmental hypoxia by living at high altitudes. In a US-wide study, people in counties located 1500 m above sea level had longer life expectancies than those within 100 m of it, by margins of 1.2-3.6 years for men and 0.5-2.5 years for women, although these associations were not significant in a multivariate analysis.[39] Nevertheless, adjusted data from the US and Switzerland associate living at a high altitude with protection against obesity and mortality from ischemic heart disease and stroke, but a higher prevalence of COPD, with all of these effects showing an altitude-dependent relationship.[39,44,45]

Our data obtained here with HIF-P4H-2-deficient (*Hif-p4h-2*$^{gt/gt}$) mice phenocopied the protection against obesity which is associated with activation of the systemic hypoxia response at high altitude. Obesity is often the cause of hepatic steatosis, which for many of the aged WT males had progressed to hepatitis, cirrhosis and even HCC. The overall better liver health of the *Hif-p4h-2*$^{gt/gt}$ males is therefore likely to be associated with their lower adiposity. Although

the number of *Hif-p4h-2*$^{gt/gt}$ mice that experienced myocardial infarctions was lower than the number of such WT mice, these infarctions were not the primary cause of death in either genotype, a fact that most likely underlines the differences in lipid metabolism between humans and mice, the latter having HDL as their most abundant lipoprotein which offers protection from severe atherosclerosis.[46,47] Where the risk of COPD is concerned, we did not detect any differences in lung architecture or fibrosis between the genotypes in the 2-year-old female mice, which would suggest that chronic HIF-P4H-2 deficiency is not a cause of COPD, although it is possible that inhibition of the other HIF-P4H isoenzymes by hypoxia, or hypoxia independently from HIF stabilization, may contribute to the higher prevalence of COPD at high altitude.[39] Moreover, we have shown earlier that the primary hepatocytes of *Hif-p4h-2*$^{gt/gt}$ mice clear ROS faster than those of the WT and have higher levels of the antioxidative glutathione,[24] which could offer the *Hif-p4h-2*$^{gt/gt}$ mice protection against diseases like COPD, where it has been proposed that ROS may be involved in their pathogenesis.[48]

Anemia, a decline in red cell counts, is associated with aged populations, leading to significant functional impairment and even to increased mortality.[49] Although there are many causes, including nutritional deficiencies and chronic diseases, anemia is also a physiological consequence of aging, when the adipose tissue replaces the hematopoietic cells in the bone marrow.[49] CKD, resulting in anemia via the loss of EPO-producing cells, is associated with obesity, type 2 diabetes and hypertension. The first-generation HIF-P4H inhibitors have been especially targeted at treating anemia, because they can also induce endogenous EPO production from the liver and regulate iron homeostasis during inflammation, the latter being associated with their ability to suppress hepatic hepcidin production.[50,51] We have shown earlier that *Hif-p4h-2*$^{gt/gt}$ mice develop splenic extramedullary erythropoiesis from 6 months onwards and that this is associated with the HIF-mediated downregulation of Notch signaling.[34] The resulting mild erythrocytosis characterized by ~20% higher hematocrit levels than in the WT was not associated with significantly increased serum or renal EPO levels.[34] We discovered here that the *Hif-p4h-2*$^{gt/gt}$ mice were protected from the aging-associated anemia seen in the WT mice. The architecture of the 2-year-old female spleens was clearly less distorted than at 1 year of age,[34] while slightly more megakaryocytes were detected than in the WT, suggestive of increased erythropoiesis in the spleen. Interestingly, the serum EPO levels of the 2-year-old *Hif-p4h-2*$^{gt/gt}$ female mice were about twice as high as those of the WT. Since the WT female kidneys were significantly more fibrotic than the *Hif-p4h-2*$^{gt/gt}$ kidneys, the protection from anemia in the *Hif-p4h-2*$^{gt/gt}$ mice most likely involved a heightened ability to maintain renal EPO production into senescence.

Hypoxia is a feature of most solid tumors that often results in HIFα stabilization, which in turn can promote cancer cell survival via induction of angiogenesis and promotion of the Warburg effect, and may induce metastasis.[12] No data exist, however, to suggest that HIF itself is oncogenic,[13] and indeed, HIF1α has also been associated with tumor suppression in several settings.[52-57] Likewise, the data on HIF-P4H-2 in cancers have been controversial. It has been reported to have both protective and exacerbating roles in lung and breast cancers, for example, and in HCC.[58-65] The data presented here would support the former, since the *Hif-p4h-2*$^{gt/gt}$ mice had less HCC, and no increase was observed in the overall incidence of cancer.

Some previous studies have found HIF1α/HIF2α stabilization to be harmful in cell or tissue type-specific settings, for example, in the case of fatty liver.[66-68] However, a full powered hypoxia response restricted to a single organ or cell type is likely to result in a different, potentially harmful outcome, from the systemic HIF-P4H-2 inhibition in the *Hif-p4h-2*$^{gt/gt}$ mice resulting in non-full powered HIF response, studied here. Although the extent of HIF-P4H-2 knockdown varies between tissues in the *Hif-p4h-2*$^{gt/gt}$ mice,[19,20] for example being only 40% in the liver where major protective phenotypes were observed, the system-wide HIF-P4H-2 inhibition induced HIF-driven metabolic reprogramming, resulting in, for example, lower adiposity, adipose tissue inflammation, and better liver health. The systemic, indirectly mediated changes in metabolism, rather than just organ-specific effects, are likely in a key-role mediating the improved tissue health observed here in many organs. Also, the overall better metabolic health, including reduced *de novo* lipogenesis, improved serum lipid profile and glucose sensitivity, reported earlier in the *Hif-p4h-2*$^{gt/gt}$ 1-year-old mice,[20] likely mediated longer-term effects contributing to the observed improved tissue health in senescence. Additionally, since longevity and slower tissue aging are associated with autophagy-promoting calorie restriction,[69] and a mild decrease in mitochondrial activity has been repeatedly shown to improve health and extend the lifespan,[70] it is likely that the major reduction in OCR and ATP production observed in the *Hif-p4h-2*$^{gt/gt}$ MEFs significantly contributes to the improved homeostasis of aged tissues.

In this study, the gender dependence of the data could not be thoroughly evaluated, since the male cohort was aged until death or a humane end point was reached, while the females were sacrificed at 2 years of age. The causes of death in the males, such as HCC or inflammatory conditions, could have had diverse effects on the systemic health of the mice, making it impossible to assess the age-dependent but disease-independent condition of their tissues. The data could nevertheless indicate potential gender-dependent differences, for example, in the health of the liver and heart, to the advantage of the aged female mice. The gender dependence of

aging would be an important issue for further studies, since differences in human aging between the sexes are recognized but not well-understood.[71]

As our study was conducted in in-bred mice, the potential contribution of modifier genes or epigenetic events is less than in an out-bred line. However, there is no reason to assume that overall findings in another background were dissimilar, while the magnitude of effect between organs might differ. In the aged *Hif-p4h-2*$^{gt/gt}$ mice the central cardiometabolic tissues, such as heart, liver, pancreas, WAT, kidney, and skeletal muscle were healthier than in the WT, especially in the males, whereas no significant difference in the health of BAT, lung or spleen were observed. Additionally, less seminal vesicle dilation, which is a common finding in older male mice, was observed in the *Hif-p4h-2*$^{gt/gt}$ mice than the WT.

In conclusion, chronic systemic HIF-P4H-2 deficiency ameliorated the homeostasis of several aged tissues including those of the liver, heart, adipose tissue, and pancreas. It did not alter the life span or lead to increased tumor formation; in fact it provided protection against HCC. These data would suggest an improved quality of life in senescence with chronic HIF-P4H-2 inhibition. Additionally, this inhibition appears to be safe, which supports the notion that the long-term use of HIF-P4H-2 inhibitors is an innocent procedure. Whether the same beneficial effects regarding aging and HCC could be obtained with the HIF-P4H therapeutic measures that are currently available[72] or under study remains to be evaluated. It should be noted that instead of HIF-P4H-2, these small molecules actually inhibit all the HIF-P4H isoenzymes.[73,74] Our data here challenge the view that long-term HIF stabilization promotes tumor development and instead associate the systemic activation of the hypoxia response with a normal life span and protection from cardiometabolic and inflammatory diseases and HCC.

ACKNOWLEDGMENTS

We thank T. Aatsinki, E. Lehtimäki, and S. Moilanen for expert technical assistance. This study was supported by Academy of Finland grants 266719 and 308009 (P. Koivunen), and 296498 (JM), the Academy of Finland Center of Excellence 2012-2017 grant 251314 (JM), and grants from the S. Jusélius Foundation (P. Koivunen and JM), the Finnish Cancer Organization (P. Koivunen), and the Jane and Aatos Erkko Foundation (P. Koivunen and JM) and FibroGen Inc. (JM). JM owns equity in FibroGen, Inc., which develops HIF-P4H inhibitors for potential therapeutic purposes and supports research headed by JM.

AUTHOR CONTRIBUTIONS

A. Laitakari, R. Huttunen, P. Hannuksela, M. Heikkilä, E.Y. Dimova, R. Serpi, and P. Koivunen performed the experiments and analyzed the data; P. Kuvaja contributed to the histological analysis of liver cancer; Z. Szabo and R. Kerkelä contributed to the liver cancer ultrasound scans; M. Heikkilä generated the mouse embryonic fibroblasts; J. Myllyharju and P. Koivunen generated the *Hif-p4h-2*$^{gt/gt}$ mouse line; P. Koivunen and A. Laitakari wrote the paper.

REFERENCES

1. Kaelin WG, Ratcliffe PJ. Oxygen sensing by metazoans: the central role of the HIF hydroxylase pathway. *Mol Cell*. 2008;30(4):393-402. https://doi.org/10.1016/j.molcel.2008.04.009
2. Loenarz C, Coleman ML, Boleininger A, et al. The hypoxia-inducible transcription factor pathway regulates oxygen sensing in the simplest animal, trichoplax adhaerens. *EMBO Rep*. 2011;12(1):63-70. Accessed February 25, 2019. https://doi.org/10.1038/embor.2010.170
3. Semenza GL. Regulation of oxygen homeostasis by hypoxia-inducible factor 1. *Physiology (Bethesda)*. 2009;24:97-106.
4. Koivunen P, Serpi R, Dimova EY. Hypoxia-inducible factor prolyl 4-hydroxylase inhibition in cardiometabolic diseases. *Pharmacol Res*. 2016;114:265-273.
5. Koivunen P, Kietzmann T. Hypoxia-inducible factor prolyl 4-hydroxylases and metabolism. *Trends Mol Med*. 2018;24(12):1021-1035. Accessed February 7, 2019. https://doi.org/10.1016/j.molmed.2018.10.004
6. Myllyharju J. Prolyl 4-hydroxylases, key enzymes in the synthesis of collagens and regulation of the response to hypoxia, and their roles as treatment targets. *Ann Med*. 2008;40(62):402-417. Accessed February 25, 2019. https://doi.org/10.1080/07853890801986594
7. Hirsilä M, Koivunen P, Günzler V, Kivirikko KI, Myllyharju J. Characterization of the human prolyl 4-hydroxylases that modify the hypoxia-inducible factor. *J Biol Chem*. 2003;278(33):30772-30780. Accessed January 8, 2019. https://doi.org/10.1074/jbc.M304982200
8. Chen N, Qian J, Chen J, et al. Phase 2 studies of oral hypoxia-inducible factor prolyl hydroxylase inhibitor FG-4592 for treatment of anemia in china. *Nephrol Dial Transplant*. 2017;32(8):1373-1386. Accessed February 25, 2019. https://doi.org/10.1093/ndt/gfx011
9. Flamme I, Oehme F, Ellinghaus P, Jeske M, Keldenich J, Thuss U. Mimicking hypoxia to treat anemia: HIF-stabilizer BAY 85-3934 (molidustat) stimulates erythropoietin production without hypertensive effects. *PLoS ONE*. 2014;9(11):e111838. Accessed February 25, 2019. https://doi.org/10.1371/journal.pone.0111838
10. Olson E, Demopoulos L, Haws TF, et al. Short-term treatment with a novel HIF-prolyl hydroxylase inhibitor (GSK1278863) failed to improve measures of performance in subjects with claudication-limited peripheral artery disease. *Vasc Med*. 2014;19(6):473-482. Accessed February 25, 2019. https://doi.org/10.1177/1358863X14557151
11. Haase VH. HIF-prolyl hydroxylases as therapeutic targets in erythropoiesis and iron metabolism. *Hemodial Int*. 2017;21(suppl 1):S110-S124. Accessed March 4, 2019. https://doi.org/10.1111/hdi.12567
12. Schito L, Semenza GL. Hypoxia-inducible factors: master regulators of cancer progression. *Trends Cancer*. 2016;2(12):758-770. Accessed March 12, 2019. https://doi.org/10.1016/j.trecan.2016.10.016
13. Kaelin WG. The VHL tumor suppressor gene: Insights into oxygen sensing and cancer. *Trans Am Clin Climatol Assoc*. 2017;128:298-307. Accessed February 25, 2019.

14. López-Otín C, Blasco MA, Partridge L, Serrano M, Kroemer G. The hallmarks of aging. *Cell*. 2013;153(6):1194-1217. Accessed February 25, 2019. https://doi.org/10.1016/j.cell.2013.05.039
15. Folgueras AR, Freitas-Rodríguez S, Velasco G, López-Otín C. Mouse models to disentangle the hallmarks of human aging. *Circ Res*. 2018;123(7):905-924. Accessed February 25, 2019. https://doi.org/10.1161/CIRCRESAHA.118.312204
16. Chang AM, Halter JB. Aging and insulin secretion. *Am J Physiol Endocrinol Metab*. 2003;284(1):7. Accessed February 25, 2019. https://doi.org/10.1152/ajpendo.00366.2002
17. McCay CM, Crowell MF, Maynard LA. The effect of retarded growth upon the length of life span and upon the ultimate body SizeOne figure. *J Nutr*. 1935;10(1):63-79. https://academic.oup.com/jn/article/10/1/63/4725662. Accessed February 25, 2019. https://doi.org/10.1093/jn/10.1.63
18. Salminen A, Kaarniranta K, Kauppinen A. Disturbed interplay between autophagy and inflammasomes. *Aging (Albany NY)*. 2012;4(3):166-175. Accessed February 25, 2019. https://doi.org/10.18632/aging.100444
19. Hyvärinen J, Hassinen IE, Sormunen R, et al. Hearts of hypoxia-inducible factor prolyl 4-hydroxylase-2 hypomorphic mice show protection against acute ischemia-reperfusion injury. *J Biol Chem*. 2010;285(18):13646-13657.
20. Rahtu-Korpela L, Karsikas S, Horkko S, et al. HIF prolyl 4-hydroxylase-2 inhibition improves glucose and lipid metabolism and protects against obesity and metabolic dysfunction. *Diabetes*. 2014;63(10):3324-3333.
21. Rahtu-Korpela L, Määttä J, Dimova EY, et al. Hypoxia-inducible factor prolyl 4-hydroxylase-2 inhibition protects against development of atherosclerosis. *Arterioscler Thromb Vasc Biol*. 2016;36(4):608-617.
22. Karsikas S, Myllymäki M, Heikkilä M, et al. HIF-P4H-2 deficiency protects against skeletal muscle ischemia-reperfusion injury. *J Mol Med*. 2016;94(3):301-310. Accessed February 25, 2019. https://doi.org/10.1007/s00109-015-1349-0
23. Kerkelä R, Karsikas S, Szabo Z, et al. Activation of hypoxia response in endothelial cells contributes to ischemic cardioprotection. *Mol Cell Biol*. 2013;33(16):3321-3329. Accessed February 25, 2019. https://doi.org/10.1128/MCB.00432-13
24. Laitakari A, Ollonen T, Kietzmann T, et al. Systemic inactivation of hypoxia-inducible factor prolyl 4-hydroxylase 2 in mice protects from alcohol-induced fatty liver disease. *Redox Biol*. 2019;22:101145. Accessed February 27, 2019. https://doi.org/10.1016/j.redox.2019.101145
25. Minamishima YA, Moslehi J, Bardeesy N, Cullen D, Bronson RT, Kaelin WG. Somatic inactivation of the PHD2 prolyl hydroxylase causes polycythemia and congestive heart failure. *Blood*. 2008;111(6):3236-3244. Accessed February 25, 2019. https://doi.org/10.1182/blood-2007-10-117812
26. Takeda K, Aguila HL, Parikh NS, et al. Regulation of adult erythropoiesis by prolyl hydroxylase domain proteins. *Blood*. 2008;111(6):3229-3235. Accessed March 13, 2019. https://doi.org/10.1182/blood-2007-09-114561
27. Snyder JM, Ward JM, Treuting PM. Cause-of-death analysis in rodent aging studies. *Vet Pathol*. 2016;53(2):233-243. Accessed February 25, 2019. https://doi.org/10.1177/0300985815610391
28. Schindelin J, Arganda-Carreras I, Frise E, et al. Fiji: An open-source platform for biological-image analysis. *Nat Methods*. 2012;9(7):676-682. Accessed February 25, 2019. https://doi.org/10.1038/nmeth.2019
29. Karsikas S, Myllymäki M, Heikkilä M, et al. HIF-P4H-2 deficiency protects against skeletal muscle ischemia-reperfusion injury. *J Mol Med*. 2016;94(3):301-310. Accessed January 8, 2019. https://doi.org/10.1007/s00109-015-1349-0
30. Cawthon RM. Telomere measurement by quantitative PCR. *Nucleic Acids Res*. 2002;30(10):e47. Accessed February 25, 2019.
31. Callicott RJ, Womack JE. Real-time PCR assay for measurement of mouse telomeres. *Comp Med*. 2006;56(1):17–22. Accessed February 25, 2019.
32. Friedewald WT, Levy RI, Fredrickson DS. Estimation of the concentration of low-density lipoprotein cholesterol in plasma, without use of the preparative ultracentrifuge. *Clin Chem*. 1972;18(6):499-502.
33. Durkin ME, Qian X, Popescu NC, Lowy DR. Isolation of mouse embryo fibroblasts. *Bio Protoc*. 2013;3(18):e908. Accessed March 15, 2019.
34. Myllymäki MNM, Määttä J, Dimova EY, et al. Notch downregulation and extramedullary erythrocytosis in hypoxia-inducible factor prolyl 4-hydroxylase 2-deficient mice. *Mol Cell Biol*. 2017;37(2). Accessed February 25, 2019. https://doi.org/10.1128/MCB.00529-16
35. Strasak AM, Rapp K, Hilbe W, et al. Serum uric acid and risk of cancer mortality in a large prospective male cohort. *Cancer Causes Control*. 2007;18(9):1021-1029. Accessed February 25, 2019. https://doi.org/10.1007/s10552-007-9043-3
36. Dovell F, Boffetta P. Serum uric acid and cancer mortality and incidence: a systematic review and meta-analysis. *Eur J Cancer Prev*. 2018;27(4):399-405. Accessed February 25, 2019. https://doi.org/10.1097/CEJ.0000000000000440
37. Zhao G, Huang L, Song M, Song Y. Baseline serum uric acid level as a predictor of cardiovascular disease related mortality and all-cause mortality: a meta-analysis of prospective studies. *Atherosclerosis*. 2013;231(1):61-68. Accessed February 25, 2019. https://doi.org/10.1016/j.atherosclerosis.2013.08.023
38. Dai Z, Li M, Wharton J, Zhu MM, Zhao Y. Prolyl-4 hydroxylase 2 (PHD2) deficiency in endothelial cells and hematopoietic cells induces obliterative vascular remodeling and severe pulmonary arterial hypertension in mice and humans through hypoxia-inducible factor-2α. *Circulation*. 2016;133(24):2447-2458. Accessed February 25, 2019. https://doi.org/10.1161/CIRCULATIONAHA.116.021494
39. Ezzati M, Horwitz MEM, Thomas DSK, et al. Altitude, life expectancy and mortality from ischaemic heart disease, stroke, COPD and cancers: national population-based analysis of US counties. *J Epidemiol Community Health*. 2012;66(7):e17. Accessed February 25, 2019. https://doi.org/10.1136/jech.2010.112938
40. Mkrtchian RI, Amiiants VI, Gromova GV, Liudinovskova RA. Sanatorium-resort treatment in a low-mountain region of patients with ischemic heart disease after aortocoronary bypass. *Kardiologiia*. 1989;29(12):22-25. Accessed March 16, 2019.
41. Mirrakhimov MM, Aĭtbaev KA, Murataliev TM, Kim NM. Possibility of correcting atherogenic dyslipoproteinemia by the mountain climate treatment. *Kardiologiia*. 1991;31(3):8-10. Accessed March 16, 2019.
42. Amiiants VI, Gromova GV, Veres AA, Bidzhieva ZN, Kazarian MA, Tolmachev VG. Changes in cardiovascular function of ischemic heart disease patients on the course of rehabilitation at low-mountain health resort after surgical revascularization of myocardium. *Klin Med (Mosk)*. 1997;75(2):26-28. Accessed March 16, 2019.

43. Hawley JA, Lundby C, Cotter JD, Burke LM. Maximizing cellular adaptation to endurance exercise in skeletal muscle. *Cell Metab*. 2018;27(5):962-976. Accessed March 15, 2019. https://doi.org/10.1016/j.cmet.2018.04.014
44. Voss JD, Masuoka P, Webber BJ, Scher AI, Atkinson RL. Association of elevation, urbanization and ambient temperature with obesity prevalence in the united states. *Int J Obes (Lond)*. 2013;37(10):1407-1412. Accessed February 7, 2019. https://doi.org/10.1038/ijo.2013.5
45. Faeh D, Gutzwiller F, Bopp M. Lower mortality from coronary heart disease and stroke at higher altitudes in Switzerland. *Circulation*. 2009;120(6):495-501. Accessed February 25, 2019. https://doi.org/10.1161/CIRCULATIONAHA.108.819250
46. Véniant MM, Zlot CH, Walzem RL, et al. Lipoprotein clearance mechanisms in LDL receptor-deficient "apo-B48-only" and "apo-B100-only" mice. *J Clin Invest*. 1998;102(8):1559-1568. Accessed March 15, 2019. https://doi.org/10.1172/JCI4164
47. Farese RV, Véniant MM, Cham CM, et al. Phenotypic analysis of mice expressing exclusively apolipoprotein B48 or apolipoprotein B100. *Proc Natl Acad Sci USA*. 1996;93(13):6393-6398. Accessed March 15, 2019.
48. Liu Z, Ren Z, Zhang J, et al. Role of ROS and nutritional antioxidants in human diseases. *Front Physiol*. 2018;9:477. Accessed March 16, 2019. https://doi.org/10.3389/fphys.2018.00477
49. Guralnik JM, Ershler WB, Schrier SL, Picozzi VJ. Anemia in the elderly: a public health crisis in hematology. *Hematolgy*. 2005:528-532. Accessed March 15, 2019. https://doi.org/10.1182/asheducation-2005.1.528
50. Provenzano R, Besarab A, Sun CH, et al. Oral hypoxia-inducible factor prolyl hydroxylase inhibitor roxadustat (FG-4592) for the treatment of anemia in patients with CKD. *Clin J Am Soc Nephrol*. 2016;11(6):982-991. Accessed March 16, 2019. https://doi.org/10.2215/CJN.06890615
51. Provenzano R, Besarab A, Wright S, et al. Roxadustat (FG-4592) versus epoetin alfa for anemia in patients receiving maintenance hemodialysis: a phase 2, randomized, 6- to 19-week, open-label, active-comparator, dose-ranging, safety and exploratory efficacy study. *Am J Kidney Dis*. 2016;67(6):912-924. Accessed March 16, 2019. https://doi.org/10.1053/j.ajkd.2015.12.020
52. Koivunen P, Lee S, Duncan CG, et al. Transformation by the (R)-enantiomer of 2-hydroxyglutarate linked to EGLN activation. *Nature*. 2012;483(7390):484-488. Accessed March 15, 2019. https://doi.org/10.1038/nature10898
53. Acker T, Diez-Juan A, Aragones J, et al. Genetic evidence for a tumor suppressor role of HIF-2alpha. *Cancer Cell*. 2005;8(2):131-141. Accessed March 15, 2019. https://doi.org/10.1016/j.ccr.2005.07.003
54. Mack FA, Rathmell WK, Arsham AM, Gnarra J, Keith B, Simon MC. Loss of pVHL is sufficient to cause HIF dysregulation in primary cells but does not promote tumor growth. *Cancer Cell*. 2003;3(1):75-88. Accessed March 15, 2019.
55. Carmeliet P, Dor Y, Herber J-M, et al. Role of HIF-1α in hypoxiamediated apoptosis, cell proliferation and tumour angiogenesis. *Nature*. 1998;394(6692):485-490. Accessed March 7, 2019. https://doi.org/10.1038/28867
56. Blouw B, Song H, Tihan T, et al. The hypoxic response of tumors is dependent on their microenvironment. *Cancer Cell*. 2003;4(2):133-146. Accessed March 16, 2019.
57. Song L-P, Zhang J, Wu S-F, et al. Hypoxia-inducible factor-1alpha-induced differentiation of myeloid leukemic cells is its transcriptional activity independent. *Oncogene*. 2008;27(4):519-527. Accessed July 13, 2019. https://doi.org/10.1038/sj.onc.1210670
58. Andersen S, Donnem T, Stenvold H, et al. Overexpression of the HIF hydroxylases PHD1, PHD2, PHD3 and FIH are individually and collectively unfavorable prognosticators for NSCLC survival. *PLoS ONE*. 2011;6(8):e23847. Accessed July 13, 2019. https://doi.org/10.1371/journal.pone.0023847
59. Bogaerts E, Paridaens A, Verhelst X, et al. Effect of prolyl hydroxylase domain 2 haplodeficiency on liver progenitor cell characteristics in early mouse hepatocarcinogenesis. *EXCLI J*. 2016;15:687. Accessed April 1, 2019.
60. Zhen L, Shijie N, Shuijun Z. Tumor PHD2 expression is correlated with clinical features and prognosis of patients with HCC receiving liver resection. *Med (United States)*. 2014;93(29):e179. Accessed April 1, 2019. https://doi.org/10.1097/MD.0000000000000179
61. Tao Y, Lin F, Li R, Shen J, Wang Z. Prolyl hydroxylase-2 inhibits its liver tumor cell proliferation and cyclin D1 expression in a hydroxylase-dependent manner. *Int J Biochem Cell Biol*. 2016;77:129-140. Accessed April 1, 2019. https://doi.org/10.1016/j.biocel.2016.05.022
62. Kuchnio A, Moens S, Bruning U, et al. The cancer cell oxygen sensor PHD2 promotes metastasis via activation of cancer-associated fibroblasts. *Cell Rep*. 2015;12(6):992-1005. Accessed April 4, 2019. https://doi.org/10.1016/j.celrep.2015.07.010
63. Di Conza G, Trusso Cafarello S, Zheng X, Zhang Q, Mazzone M. PHD2 targeting overcomes breast cancer cell death upon glucose starvation in a PP2A/B55α-mediated manner. *Cell Rep*. 2017;18(12):2836-2844. Accessed April 4, 2019. https://doi.org/10.1016/j.celrep.2017.02.081
64. Kozlova N, Wottawa M, Katschinski DM, Kristiansen G, Kietzmann T. Hypoxia-inducible factor prolyl hydroxylase 2 (PHD2) is a direct regulator of epidermal growth factor receptor (EGFR) signaling in breast cancer. *Oncotarget*. 2017;8(6):9885-9898. Accessed April 4, 2019. https://doi.org/10.18632/oncotarget.14241
65. Klotzsche-Von Ameln A, Muschter A, Mamlouk S, et al. Inhibition of HIF prolyl hydroxylase-2 blocks tumor growth in mice through the antiproliferative activity of TGFβ. *Cancer Res*. 2011;71(9):3306-3316. Accessed April 4, 2019. https://doi.org/10.1158/0008-5472.CAN-10-3838
66. Nath B, Levin I, Csak T, et al. Hepatocyte-specific hypoxia-inducible factor-1α is a determinant of lipid accumulation and liver injury in alcohol-induced steatosis in mice. *Hepatology*. 2011;53(5):1526-1537. Accessed April 17, 2019. https://doi.org/10.1002/hep.24256
67. Rankin EB, Rha J, Selak MA, et al. Hypoxia-inducible factor 2 regulates hepatic lipid metabolism. *Mol Cell Biol*. 2009;29(16):4527-4538. Accessed April 1, 2019. https://doi.org/10.1128/MCB.00200-09
68. Xie C, Yagai T, Luo Y, et al. Activation of intestinal hypoxia-inducible factor 2α during obesity contributes to hepatic steatosis. *Nat Med*. 2017;23(11):1298-1308. Accessed April 1, 2019. https://doi.org/10.1038/nm.4412
69. Bagherniya M, Butler AE, Barreto GE, Sahebkar A. The effect of fasting or calorie restriction on autophagy induction: a review of the literature. *Ageing Res Rev*. 2018;47:183-197. Accessed February 7, 2020. https://doi.org/10.1016/j.arr.2018.08.004
70. Hwang AB, Jeong D, Lee S. Mitochondria and organismal longevity. *Curr Genomics*. 2012;13(7):519-532. Accessed February 7, 2020. https://doi.org/10.2174/138920212803251427

71. Austad SN, Fischer KE. Sex differences in lifespan. *Cell Metab*. 2016;23(6):1022-1033. Accessed June 26, 2019. https://doi.org/10.1016/j.cmet.2016.05.019
72. Dhillon S. Roxadustat: first global approval. *Drugs*. 2019;79(5):563-572. Accessed June 26, 2019. https://doi.org/10.1007/s40265-019-01077-1
73. Laitala A, Aro E, Walkinshaw G, et al. Transmembrane prolyl 4-hydroxylase is a fourth prolyl 4-hydroxylase regulating EPO production and erythropoiesis. *Blood*. 2012;120(16):3336-3344. Accessed March 13, 2019. https://doi.org/10.1182/blood-2012-07-441824
74. Yeh T, Leissing TM, Abboud MI, et al. Molecular and cellular mechanisms of HIF prolyl hydroxylase inhibitors in clinical trials. *Chem Sci*. 2017;8(11):7651-7668. Accessed March 14, 2019. https://doi.org/10.1039/c7sc02103h

SUPPORTING INFORMATION

Additional Supporting Information may be found online in the Supporting Information section.
Supinfo

How to cite this article: Laitakari A, Huttunen R, Kuvaja P, et al. Systemic long-term inactivation of hypoxia-inducible factor prolyl 4-hydroxylase 2 ameliorates aging-induced changes in mice without affecting their life span. *The FASEB Journal*. 2020;00:1–20. https://doi.org/10.1096/fj.201902331R